

Dynamical Dark Matter: I. Theoretical Overview

Keith R. Dienes^{1,2,3*}, Brooks Thomas^{4†}

¹ *Physics Division, National Science Foundation, Arlington, VA 22230 USA*

² *Department of Physics, University of Maryland, College Park, MD 20742 USA*

³ *Department of Physics, University of Arizona, Tucson, AZ 85721 USA*

⁴ *Department of Physics, University of Hawaii, Honolulu, HI 96822 USA*

In this paper, we propose a new framework for dark-matter physics. Rather than focus on one or more stable dark-matter particles, we instead consider a multi-component framework in which the dark matter of the universe comprises a vast ensemble of interacting fields with a variety of different masses, mixings, and abundances. Moreover, rather than impose stability for each field individually, we ensure the phenomenological viability of such a scenario by requiring that those states with larger masses and Standard-Model decay widths have correspondingly smaller relic abundances, and vice versa. In other words, dark-matter stability is not an absolute requirement in such a framework, but is balanced against abundance. This leads to a highly dynamical scenario in which cosmological quantities such as Ω_{CDM} experience non-trivial time-dependences beyond those associated with the expansion of the universe. Although it may seem difficult to arrange an ensemble of states which have the required decay widths and relic abundances, we present one particular example in which this balancing act occurs naturally: an infinite tower of Kaluza-Klein (KK) states living in the bulk of large extra spacetime dimensions. Remarkably, this remains true even if the stability of the KK tower itself is entirely unprotected. Thus theories with large extra dimensions — and by extension, certain limits of string theory — naturally give rise to dynamical dark matter. Such scenarios also generically give rise to a rich set of collider and astrophysical phenomena which transcend those usually associated with dark matter.

I. INTRODUCTION, MOTIVATION, AND SUMMARY

Situated at the nexus of particle physics, astrophysics, and cosmology lies one of the most compelling mysteries that faces physics today: that of unravelling the identity and properties of dark matter [1]. From measurements of galactic rotation curves and velocity dispersions to observations of the gravitational lensing of galaxy clusters and the detection of specific acoustic peaks of the cosmic microwave background (CMB), ample circumstantial evidence suggests that most of the matter in the universe does not interact strongly or electromagnetically. Such matter is therefore electrically neutral (dark) and presumed non-relativistic (cold). Beyond these properties, however, very little is known about the nature of dark matter. Fortunately, the current generation of dark-matter experiments have unparalleled sensitivities, and new data concerning the possible direct and indirect detection of dark matter can be expected soon. This data will therefore go a long way towards not only resolving this pressing cosmological mystery, but also constraining the possibilities for physics beyond the Standard Model (SM).

Many theoretical proposals for physics beyond the Standard Model give rise to suitable dark-matter candidates. However, most of these dark-matter candidates consist of a single particle (or a small collection of par-

ticles) which are stable on cosmological time scales as the result of a discrete symmetry. Examples include the lightest supersymmetric particle (LSP) in supersymmetric theories, and the lightest Kaluza-Klein particle (LKP) in certain higher-dimensional theories in which the Standard Model propagates in the bulk [2]. In the first case, the LSP is stabilized by the assumption of an R -parity symmetry, while in the second case the stabilizing symmetry is a so-called “KK parity”. However, in all cases, the ability of these particles to serve as dark-matter candidates rests squarely on their stability. Indeed, any particle which decays into Standard-Model states too rapidly is likely to upset traditional big-bang nucleosynthesis (BBN) and its successful predictions of light-element abundances. Such decays can also leave unacceptable imprints in the cosmic microwave background and diffuse X-ray and gamma-ray backgrounds. For this reason, stability is often the very first criterion required for the phenomenological success of a hypothetical dark-matter candidate.

There is, of course, one important exception to this argument: a given dark-matter particle need not be stable if its abundance at the time of its decay is sufficiently small. A sufficiently small abundance ensures that the disruptive effects of the decay of such a particle will be minimal, and that all constraints from BBN, the CMB, *etc.*, will continue to be satisfied.

In this paper, we shall consider a new framework for dark-matter physics which takes advantage of this possibility. Specifically, we shall consider a multi-component framework in which the dark matter of the universe comprises a vast ensemble of interacting fields with a variety of different masses, mixings, and abundances. Rather

*E-mail address: dienes@physics.arizona.edu

†E-mail address: thomasbd@phys.hawaii.edu

than impose stability for each field individually (or even for the ensemble of fields as a whole), we shall ensure the phenomenological viability of such a scenario by requiring that those states with larger masses and larger decay widths into Standard-Model fields have correspondingly smaller relic abundances, and vice versa. In other words, dark-matter stability is not an absolute requirement in such a framework, but is balanced against abundance. As we shall demonstrate, this leads to a highly dynamical scenario in which cosmological quantities such as Ω_{CDM} experience non-trivial time-dependences beyond those associated with the expansion of the universe. We shall therefore refer to such a scenario as “dynamical dark matter”.

In general, it might seem difficult (or at best fine-tuned) to have an ensemble of states which are not only suitable candidates for dark matter but in which the abundances and decay widths are precisely balanced in this manner. However, it turns out that theories with large extra spacetime dimensions not only naturally provide such ensembles of states, but do so in a manner which is virtually intrinsic to their construction. If the Standard Model is restricted to a brane floating in a higher-dimensional space, it then immediately follows that any field propagating in the bulk of this space must be neutral under all Standard-Model symmetries. As a consequence, such bulk fields can have at most gravitational interactions with the physics on the brane, and will therefore appear as dark matter from the perspective of an observer on the brane. Moreover, from the perspective of this four-dimensional observer, such bulk fields will appear as an infinite tower of individual Kaluza-Klein (KK) modes. This, then, would constitute our dark-matter ensemble.

At first glance, such a scenario for dark matter would appear to face a major phenomenological hurdle: in the absence of additional symmetries or *ad-hoc* assumptions, an entire Kaluza-Klein tower of bulk states will generally be unstable: the heavy KK states in such a tower will generically decay into not only lighter KK bulk states but also Standard-Model brane states, and the lighter KK states will also decay into Standard-Model brane states. Even the stability of the lightest modes of the bulk field is not guaranteed. This instability of the Kaluza-Klein tower therefore appears to pose a serious threat for the survival of big-bang nucleosynthesis in its traditional form, and can similarly disturb the X-ray and gamma-ray backgrounds.

Fortunately, there are two critical features of Kaluza-Klein towers which can play off against each other in order to render such a scenario phenomenologically viable. As one goes higher and higher in a generic KK tower, it is true that the decay width of the KK states generally increases with the KK mass. However, it is also true that the cosmological abundance associated with such states can often *decrease* with the KK mass. This is particularly true if we imagine that these states are cosmologically produced through misalignment production, as turns out

to be particularly appropriate for such scenarios. As a result, it might be possible that all KK states which decay before or during BBN have such small abundances that the destructive effects of their decays are insignificant, while at the same time a significant fraction of the KK tower survives to the present day and thereby contributes to the observed total dark-matter abundance. Thus, the surviving dark matter at the present day would consist of not merely one or two states, but a significant fraction of an entire interacting KK tower. Through the existence of such “dark towers”, theories of large extra spacetime dimensions therefore provide an ideal realization of our general dynamical dark-matter scenario.

In this paper, we shall lay out the general properties of such a scenario and explore the extent to which such a scenario is viable. Moreover, we shall attempt to do so in a completely model-independent way, without making any assumption concerning the nature of the bulk field in question. However, it is important to recognize that this entire approach represents a somewhat unorthodox approach to dark-matter physics. By balancing the stability of the different dark-matter components against their abundances across a large or even infinite ensemble, the dark matter in this scenario is intrinsically *dynamical* — its different components continue to experience non-trivial mixings and decays throughout their cosmological evolution, with such dynamical behavior continuing until, during, and beyond the current epoch. Moreover, because the dark matter in our scenario has multiple components, its phenomenology cannot be characterized in terms of a single mass or annihilation cross-section. This can therefore lead to an entirely new dark-matter phenomenology, profoundly changing the way in which such dark matter might be observed and constrained through collider experiments and astrophysical observations. Indeed, within the specific context of large extra dimensions, we shall see that one important new phenomenon that emerges for such dark matter is the possibility of “decoherence” — *i.e.*, the phenomenon in which only a single linear combination of KK modes couples to brane physics at one instant before decohering and becoming essentially invisible to the brane at all subsequent times.

It is also important that this framework not be confused with recent proposals concerning so-called “Kaluza-Klein dark matter” [2]. Theories of KK dark matter require that the entire Standard Model propagate in the large extra dimensions [3–5], and that the lowest excited KK mode of a Standard-Model field (such as the lowest-excited KK photon or neutrino) be stable as the result of an internal geometric symmetry such as KK parity [2, 5]. Such theories of KK dark matter are therefore similar to theories of supersymmetric dark matter — they are theories of a single, stable, dark-matter particle. While phenomenologically consistent, such a point of view is diametrically opposed to what we are suggesting here. Moreover, in doing away with the infinite tower of KK states and focusing exclusively on the single lightest KK mode, such “KK dark matter” theories also do

away with that part of the physics which is intrinsically higher-dimensional. The resulting scenarios are therefore insensitive to the rich physics that can emerge from an entire tower of Kaluza-Klein states acting in unison, with non-trivial masses and mixings governing their dynamics. Indeed, it is precisely such behavior that would give a window into the nature of the extra dimensions from which such states emerge.

By contrast, because our scenario balances a spectrum of decay lifetimes against a spectrum of relic abundances, our framework is sensitive to the physics of the entire tower of KK states and thereby makes use of the full higher-dimensional “bulk” in a fully higher-dimensional way. Moreover, since Type I string theories naturally give rise to closed-string states (such as the graviton, various moduli, and axions) which live in more spacetime dimensions than the Standard-Model open-string states which are restricted to live on D-branes, the scenario we shall be investigating is also extremely natural — and indeed almost unavoidable — in certain limits of string theory. Our work can therefore be seen as providing a test of the extent to which such string theories remain cosmologically viable as a function of the volume of the extra dimensions transverse to the Standard-Model brane. In other words, by studying dynamical dark matter and its phenomenological viability, we are not only exploring a new candidate for dark matter but also providing new phenomenological constraints on large extra dimensions and certain limits of string theory.

This paper is organized as follows. In Sect. II, we shall introduce our dynamical dark-matter framework in its most general form, without making reference to the specific example of large extra dimensions or KK towers. We shall discuss how lifetimes and abundances can play off against each other in such a scenario, and sketch the resulting contributions to the total dark-matter abundance as they evolve in time. In Sect. III, we shall then focus on the example of a generic tower of Kaluza-Klein states emerging from the bulk of large extra dimensions, and show that such a tower has all the required properties to be a dynamical dark-matter candidate, with abundances and lifetimes that satisfy unique mathematical inverse relations. We shall then proceed, in Sect. IV, to discuss several laboratory and astrophysical signatures of such a scenario, focusing on those new features which transcend typical dark-matter signatures and which might explain why such dark matter has not yet been observed. Throughout this paper, our analysis shall be as general as possible without specifying the precise nature of the bulk field in question. We shall then conclude in Sect. V with a discussion of extensions and possible generalizations of our dark-matter framework.

This paper is the first in a two-part series. The primary purpose of the present paper is merely to provide a general theoretical overview of the dynamical dark-matter framework. As a result, we will not choose a particular species of dark-matter field, neither restricting ourselves to specific numbers nor subjecting ourselves to specific

phenomenological bounds. Instead, our discussion here will focus on the full range of theoretical possibilities afforded by this new scenario. However, in a companion paper [6] we will provide a detailed “proof of concept” by focusing on the particular case that the KK bulk field in question is an axion. In particular, in Ref. [6] we will demonstrate that a bulk axion field can satisfy all theoretical and numerical constraints needed to serve as a dynamical dark-matter candidate, and moreover we will demonstrate that this candidate also satisfies all known cosmological, astrophysical, and collider bounds on dark matter. Indeed, in making this assertion, Ref. [6] will borrow heavily from the results of a third paper [7], a detailed forthcoming phenomenological study of axions and axion-like particles in higher dimensions. Thus, taken together, these papers will demonstrate that our dynamical dark-matter scenario remains a very real possibility for explaining the dark matter of the universe.

II. DYNAMICAL DARK MATTER: GENERAL SCENARIO

In this section we shall begin by discussing our dynamical dark-matter scenario in its most general form, without reference to specific examples such as those involving extra spacetime dimensions or KK towers of bulk fields.

A. Γ versus Ω : Balancing lifetimes against abundances

Broadly speaking, upon positing any new scenario for dark matter, one faces certain immediate constraints which must be satisfied. These constraints ultimately restrict either the abundance of the dark matter, the lifetime of the dark matter, or the relation between the two.

Let us begin by considering the case of a single dark-matter particle χ . Since this dark-matter particle is presumed unique, it alone must carry the entire observed dark-matter abundance: $\Omega_\chi = \Omega_{\text{CDM}} \approx 0.23$ [8]. However, given this large abundance, consistency with constraints coming from big-bang nucleosynthesis, the cosmic microwave background, and diffuse X-ray and gamma-ray backgrounds together require that χ have a lifetime which meets or exceeds the current age of the universe. Otherwise, decays of χ run the risk of disturbing BBN and its successful predictions for light-element abundances. Such early decays also have the potential to distort the cosmic microwave background as well as the X-ray and gamma-ray backgrounds.

However, because of the quantum-mechanical nature of the decay process, not all dark matter will decay at once. As a result, the lifetime of χ must actually *exceed* the age of the universe by at least one or two orders of magnitude in order to ensure that χ has a negligible chance of having already decayed in the recent past. This

likewise implies that such a particle also has a negligible chance of decaying either today or tomorrow. Such a particle χ is therefore “hyper-stable”. Indeed, this is the case for most if not all known single-particle dark-matter candidates.

Hyper-stability is the only way in which a single-particle dark-matter candidate can satisfy the competing constraints of having a significant abundance $\Omega_\chi \sim \Omega_{\text{CDM}}$ while simultaneously avoiding the dangerous effects of decaying into Standard-Model particles. This then results in a dark-matter scenario which is “frozen” in time, with cosmological quantities such as Ω_χ evolving only because of the expansion of the universe.

However, the primary purpose of this paper is to propose that there is another way — a “dynamical” way — to satisfy these competing constraints. First, we recognize that in some sense, it is somewhat unnatural to consider the dark matter of the universe as consisting of only a single particle. After all, the *visible* matter of the universe constitutes only a small fraction of the energy density attributed to dark matter, and yet is teeming with a diversity and complexity, known as the Standard Model, in which a complex network of elementary particles is organized according to their own internal principles. It therefore seems natural to consider the new opportunities that are open to us by taking the dark matter to consist of multiple particles as well.

In this paper, we shall therefore imagine that the dark matter consists of a vast ensemble of particles χ_i , $i = 1, 2, \dots, N$ with $N \gg 1$. The first observation that follows from this assumption is that none of these particles individually needs to have a significant abundance, since they may still *collectively* yield the correct total abundance Ω_{CDM} . As a special case, for example, we might imagine that each particle χ_i shares a common abundance $\Omega_i = \Omega_{\text{CDM}}/N$. However, if these particles were also to have equal lifetimes, then this would not solve our second constraint — that of protecting the successes of BBN and minimally impacting the CMB and other diffuse backgrounds — unless each of these particles is not only stable but hyper-stable. This is because the net effect of the nearly simultaneous decays of each of these N particles would be no different than that of the decay of a single particle carrying the full abundance Ω_{CDM} .

However, the fact that we have multiple particles furnishes us with an alternate way to satisfy these constraints: we can imagine that each of these particles has a significantly *different* lifetime. In general, these particles can also have different individual abundances. As long as those particles which have relatively short lifetimes also have correspondingly small abundances, and as long as those particles which have relatively large abundances also have relatively long lifetimes, we can reproduce the correct total dark-matter abundance Ω_{CDM} while simultaneously avoiding any damaging effects on BBN, the CMB, etc. In this way, the existence of a vast ensemble of dark-matter particles χ_i opens up the possibility of balancing abundances against decay widths in a non-

trivial way across a multitude of states.

This, then, is the essence of our dynamical dark-matter proposal. The fact that we have distributed the total required dark-matter abundance across many states means that no particular state is forced to carry a significant abundance on its own. We thus have the room to give these states a whole spectrum of lifetimes (or decay widths) without running afoul of cosmological constraints.

Note that the usual scenario of a single hyper-stable dark-matter particle is nothing but a special case of this more general framework: even though our scenario has $N \gg 1$, it still remains possible that one particle (or just a few particles) could carry the bulk of the abundance Ω_{CDM} at the present time. Following the same logic that applied in the single-particle case, this small subset of states would then be required to be hyper-stable, and all of the remaining states would have abundances that are far too insignificant to be of consequence. However, the novel features of our scenario emerge in the opposite limit, when we imagine that *none* of our dark-matter states individually carries the bulk of the total relic abundance. Some fraction of these states then no longer need to be hyper-stable, leading to a dynamical scenario in which spontaneous dark-matter decays are occurring prior to, during, and beyond the current epoch. As a result of this behavior, cosmological quantities such as Ω_{CDM} will experience time-variations which transcend those due to the ordinary expansion of the universe.

B. Dynamical dark matter: Time-evolution of individual components

It is possible to outline the salient features of this scenario somewhat more quantitatively without loss of generality. For this purpose, we shall describe the history of the universe as progressing through four distinct eras respectively associated with inflation (vacuum domination), reheating (RH), radiation domination (RD), and matter domination (MD). Note that the reheating era is itself essentially matter-dominated, with the matter in this case consisting of the oscillating inflaton. Likewise, note that even though the current epoch is technically a Λ CDM universe, approximating this epoch as matter-dominated is nevertheless a fairly good approximation. For the purposes of our general discussion, we shall not specify the particular energy or temperature scales associated with the transitions between these eras; such scales, especially as they relate to inflation and reheating, are likely to be highly model-dependent. However, regardless of these energy scales, a quantity whose energy density ρ and pressure p are related through a single-parameter equation of state of the form $p = w\rho$ will have a relative relic abundance $\Omega \equiv \rho/\rho_{\text{crit}}$ that scales as a

function of cosmological time t according to¹

$$\Omega \sim \begin{cases} t^{(1-3w)/2} & \text{RD era} \\ t^{-2w} & \text{RH/MD eras} \\ \exp[-3H(1+w)t] & \text{inflationary era.} \end{cases} \quad (1)$$

Recall that $w = 0$ for matter, while $w = -1$ for vacuum energy (cosmological constant) and $w = \pm 1/3$ for radiation and curvature respectively.

For concreteness, we shall assume that the individual components of the eventual dark matter in our scenario are described by scalar fields ϕ_i with corresponding masses m_i and widths Γ_i describing their decays into Standard-Model states. For simplicity we shall also assume that these widths Γ_i correspond to processes in which a given dark-matter component ϕ_i decays *directly* into SM states (*i.e.*, $\phi_i \rightarrow \text{SM}$) without passing through any other dark-matter components as intermediate states. In other words, we shall assume that *extra-ensemble* decays $\phi_i \rightarrow \text{SM}$ (with combined total width Γ_i) dominate over all possible *intra-ensemble* decays $\phi_i \rightarrow \phi_j + \dots$. It turns out that this is a valid assumption for many realistic scenarios to be discussed in this paper and in Ref. [6], and in the Appendix we shall discuss what happens when this assumption is relaxed.

In a Friedmann-Robertson-Walker (FRW) cosmology parametrized by a Hubble parameter $H(t) \sim t^{-1}$ in which we assume that our dark-matter component fields ϕ_i have negligible spatial variations as well as negligible self-interactions, these fields will time-evolve according to the differential equation

$$\ddot{\phi}_i + [3H(t) + \Gamma_i]\dot{\phi}_i + m_i^2\phi_i = 0. \quad (2)$$

This is the equation for a damped harmonic oscillator, with critical damping occurring for $3H(t) + \Gamma_i = 2m_i$; note that the single-derivative “friction” term in this equation receives two separate contributions, one arising from the cosmological Hubble expansion and the other arising from the intrinsic decay of ϕ_i . As a result, at early times for which $3H(t) + \Gamma_i > 2m_i$, the field ϕ_i is overdamped: it does not oscillate, and consequently its energy density behaves like vacuum energy (with $w = -1$). By contrast, at later times for which $3H(t) + \Gamma_i < 2m_i$, the field is underdamped: it therefore oscillates, and consequently its energy density scales appropriately for matter (with $w = 0$). The condition $3H(t) + \Gamma_i = 2m_i$ thus describes the “turn-on” time at which oscillatory behavior begins and the field begins to act as true matter.

Given these observations, we can now sketch how each of the abundances Ω_i for each component ϕ_i will behave

in our scenario. For concreteness, we shall assume that these abundances are all initially established at a common time t_0 . Moreover, we shall assume that each component has an initial abundance which decreases as a function of its mass. While not all production mechanisms have this property, we shall see in Sect. III that misalignment production in particular can accomplish this task.

Immediately upon establishment of these abundances, the states in our ensemble can be separated into two groups. Those heavier states with masses $3H(t_0) + \Gamma_i < 2m_i$ will all begin oscillating simultaneously. In other words, they experience a simultaneous, instantaneous turn-on. By contrast, the lighter states with $3H(t_0) + \Gamma_i > 2m_i$ will experience a step-by-step “staggered” turn-on, with lighter and lighter states crossing the turn-on threshold at later and later times. Indeed, if we approximate $H(t) \approx \kappa/3t$ where κ is a constant within each era, then a given mode with mass m_i will turn on at a time $t_i \approx \kappa/2m_i$. Thus the lightest states are necessarily the last to turn on. Indeed, $\kappa = 2$ for the RH and MD eras, while $\kappa = 3/2$ for the RD era.

Finally, once these states are all “turned on” and behave as matter with $w = 0$, their abundances Ω_i will evolve as discussed above until such times $t \sim \tau_i \equiv \Gamma_i^{-1}$ as these states decay. Specifically, the abundance $\Omega_i \sim \rho_i/H^2$ associated with each component ϕ_i will evolve according to the differential equation

$$\dot{\Omega}_i + \left(3H + 2\frac{\dot{H}}{H} + \Gamma_i\right) \Omega_i = 0. \quad (3)$$

[This equation follows directly from Eq. (2) upon use of the general expression $\rho_i = \frac{1}{2}(m_i^2\phi_i^2 + \dot{\phi}_i^2)$ and the virial theorem $m_i^2\phi_i^2 = \dot{\phi}_i^2$, the latter holding for oscillations whose frequencies are large compared with Γ_i .] Note that if we ignore the decays of these particles (*i.e.*, if we set $\Gamma_i \rightarrow 0$), the solutions to this differential equation are nothing but the results given in Eq. (1) for $w = 0$. Upon decay, however, the corresponding abundance Ω_i drops rapidly to zero; this occurs when $t \sim \tau_i$, and indeed $\Gamma_i \gtrsim 3H + 2\dot{H}/H$ at $t \sim \tau_i$. For simplicity, in the rest of this paper we shall approximate such decays as occurring promptly and completely at $t = \tau_i$. However this approximation will not be critical for any of our conclusions, and can easily be discarded if needed.

Combining all these features, we can then sketch the salient features of our scenario as in Fig. 1. In this plot, we have taken the time at which the initial abundances are established to be during the inflationary era, but other time intervals are also possible. We have also assumed that $\Gamma_i \ll 3H(t_i)$ when $3H(t_i) = 2m_i$, so that the decay widths Γ_i affect the final decay times τ_i but not the staggered turn-on times t_i .

Several features which are clear from this sketch help to define and characterize this scenario. First, we see that at the present time, there continue to be a plethora of dark-matter states. Although each of these has an extremely

¹ The results in Eq. (1) follow from the general facts that $\rho \sim R^{-3(1+w)}$ and $\rho_{\text{crit}} \sim H^2$, where R and H are respectively the scale factor and Hubble parameter. Recall that these latter quantities have the scaling behaviors $(R, H) \sim (t^{1/2}, t^{-1})$ in an RD era; $(R, H) \sim (t^{2/3}, t^{-1})$ in RH or MD eras; and $(R, H) \sim (e^{Ht}, \text{constant})$ in an inflationary era.

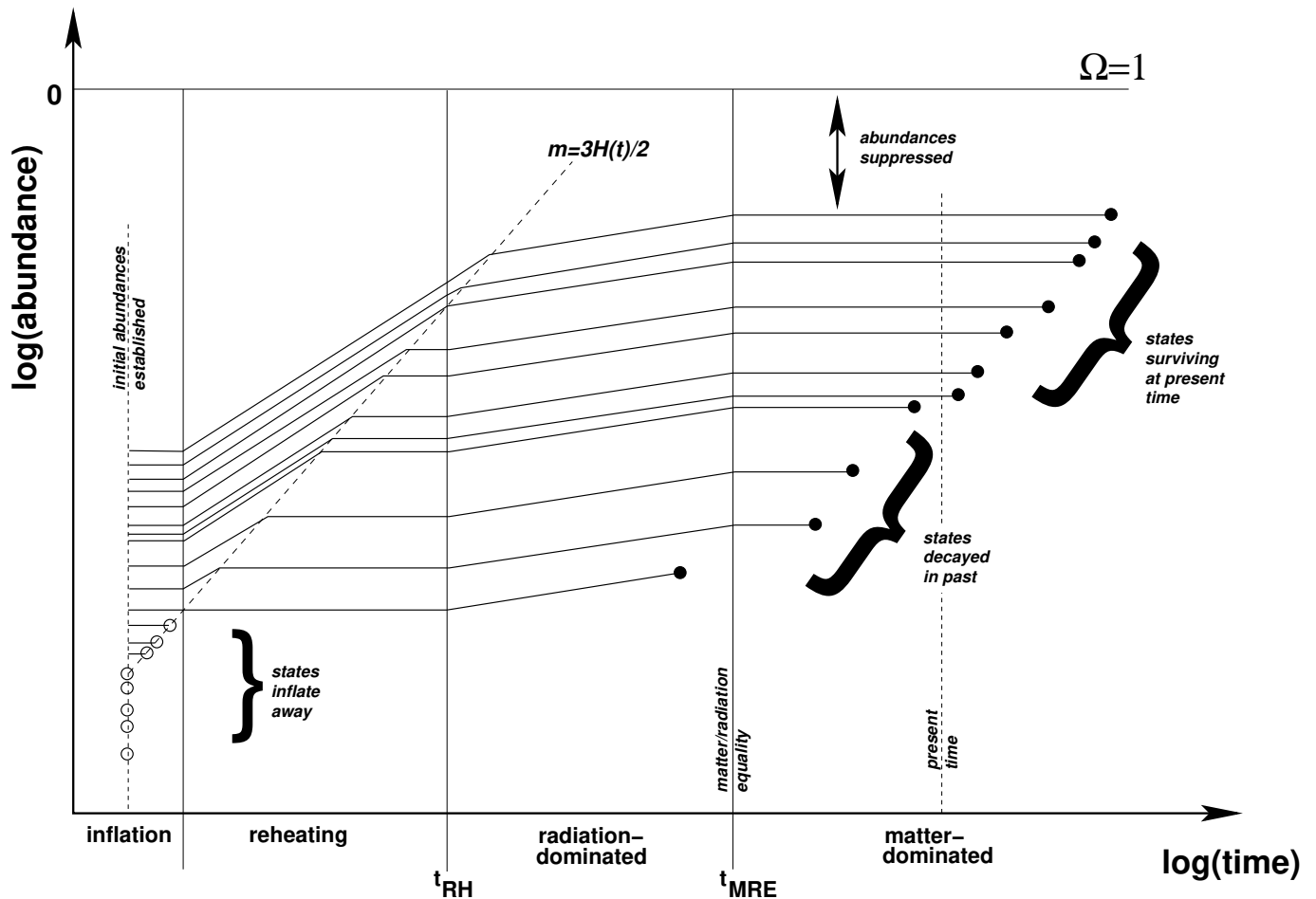


FIG. 1: A sketch of our dynamical dark-matter scenario in which the dark matter of the universe comprises a vast ensemble of individual components with different masses, abundances, and lifetimes. This plot illustrates the evolution of the abundance of each dark-matter component as a function of time, assuming that all abundances are initially established at a common time (chosen here to be prior to or during the inflationary era), with values that decrease as a function of the component mass. For all subsequent times, these abundances scale as vacuum energy until $3H(t) = 2m_i$, after which point they scale as matter. Open circles indicate states which inflate away, while closed circles indicate states which decay into SM particles with associated lifetimes that decrease with increasing mass. In our scenario, the lifetimes and abundances are balanced against each other in such a way that there continue to exist a plethora of dark-matter states which survive at the present time: although each such state has an extremely small abundance $\Omega_i \ll 1$, they collectively reproduce Ω_{CDM} . Nevertheless, because of their extremely small abundances, states which have already decayed into SM particles leave negligible imprints on the CMB and other observable astrophysical and cosmological backgrounds. An important feature of this scenario is that it is fully *dynamical*, with the composition and properties of the dark matter continuing to experience a non-trivial time evolution before, during, and even after the current epoch.

small abundance (exponentially suppressed on the plot in Fig. 1), they can collectively produce a sizable, $\mathcal{O}(1)$ abundance which we choose to identify with the observed dark-matter abundance $\Omega_{\text{CDM}} \approx 0.23$ [8].

Second, we observe that our dark-matter states are not governed by the notion of stability: while some are indeed more stable than others, decays of dark-matter states can occur *throughout* the evolution of the universe. This is not in conflict with observational constraints because of the extremely small abundances of those states which decay at critical epochs during the evolution of the universe. In other words, as discussed above, lifetimes and abun-

dances are balanced against each other in this scenario.

Third, as a consequence of these features, we see that nothing is particularly special about the present time in this framework. Dark-matter states need not be held stable until any special moment, and the current age of the universe plays no special role in this scenario. Indeed, as evident from the sketch in Fig. 1, dark-matter states decay prior to, during, and after the present era. What results, then, is a scenario in which the dark matter is not frozen in time at the present era, but continues to act as a highly dynamical component of an ever-evolving universe.

C. Characterizing a given dark-matter configuration: Ω_{tot} , η , and w_{eff}

In general, there are three quantities which we can use in order to characterize the configuration of our dark-matter ensemble at any instant in time, and to track its subsequent time-evolution. We shall begin by introducing these three quantities and discussing the relations between them. Then, we shall discuss several qualitative aspects of their overall time-evolutions.

1. Fundamental definitions and relations

The first quantity we shall define in order to characterize the configuration of our dark-matter ensemble is the total dark-matter abundance:

$$\Omega_{\text{tot}} \equiv \sum_i \Omega_i . \quad (4)$$

Note that we should include in this sum the contributions from only those components in our ensemble which have already “turned on” (*i.e.*, have begun oscillating) and which are therefore already behaving as true matter. Restricting such contributions in this way ensures that Ω_{tot} can truly be associated with a total dark-matter abundance. Of course, all of the components in our ensemble will eventually “turn on” and behave as dark matter after enough time has passed. It is for this reason that we shall continue to refer to each component of our ensemble as a dark-matter component, regardless of its particular turn-on time.

The quantity Ω_{tot} describes the total dark-matter abundance at any instant of time. However, we may also define a complementary quantity η which describes how this total abundance is *distributed* across the different components:

$$\eta \equiv 1 - \frac{\Omega_0}{\Omega_{\text{tot}}} . \quad (5)$$

Here $\Omega_0 \equiv \max_i \{\Omega_i\}$ is defined to be the largest individual dark-matter abundance from amongst our ensemble of dark-matter states. Thus, η measures what fraction of the total abundance Ω_{tot} is *not* carried by a single dominant component. We see from its definition that η varies within the range $0 \leq \eta \leq 1$: values of η near zero signify the traditional situation in which the total dark-matter abundance is predominantly carried by a single state, while larger values of η signify departures from this traditional configuration. In this sense, then, η can also be viewed as quantifying the degree to which our scenario deviates from the more traditional dark-matter framework at any instant in time.

Recall that we have assumed for this discussion that the more massive components of our ensemble have smaller initial abundances, and vice versa. Indeed, this assumption is already reflected in the sketch in Fig. 1.

It then follows that the largest abundance Ω_0 in Eq. (5) will correspond to the lightest component in our ensemble. However, in the event of a “staggered” turn-on, the lightest components in the ensemble are necessarily the last to turn on. Indeed, prior to their turn-on times, the abundances of these lightest states contribute to the total dark-*energy* abundance rather than to the total dark-matter abundance. We must therefore be careful to identify Ω_0 as the abundance associated with the lightest of those components which have already turned on. As a result, even the identity of the component whose abundance is to be identified with Ω_0 can occasionally be time-dependent.

While both Ω_{tot} and η characterize the configuration of our dark-matter ensemble at a given instant in time, one of the critical features of our dynamical dark-matter scenario is precisely that it is *dynamical* — *i.e.*, that these quantities have non-trivial time-evolutions. Of course, some of this time-evolution is common to all dark-matter scenarios, arising due to the Hubble expansion of the universe during its reheating, radiation-dominated, or matter-dominated eras. There are, however, additional time-dependent effects which are unique to our dynamical dark-matter scenario. For example, one such effect dominates the physics of the final, matter-dominated era, and arises because the total dark-matter abundance in our scenario has been distributed across many individual dark-matter components, each with a potentially different lifetime. This phenomenon leads to a slowly falling Ω_{tot} at late times. Clearly the time-evolution of Ω_{tot} during this period is extremely sensitive to not only the distribution of the abundances Ω_i across the different dark-matter components within the ensemble, but also the decay widths Γ_i which govern the times at which these different components decay.

For this reason, it will be useful to define a quantity which can meaningfully characterize the aggregate time-evolution of our ensemble. Moreover, we would like this quantity to characterize this time-evolution regardless of the particular cosmological era under study, and likewise to quantify the extent to which this time-evolution intrinsically differs from that normally associated with the cosmological expansion of the universe.

We have already seen in Eq. (1) that the time-dependence of the abundance Ω_i associated with a *single* dark-matter component can be parametrized by its equation-of-state parameter w . It is therefore natural to ask what “effective” equation-of-state parameter w_{eff} might collectively describe our entire dynamical ensemble of dark-matter components. For example, even though each individual dark-matter component behaves as matter (with $w = 0$), the decays of these components at late times (or even their staggered turn-ons at early times) might conspire to produce an *effective* w -value for the entire ensemble which is non-zero. Such behavior is illustrated in Fig. 2 for decays that occur during the final matter-dominated era. In all cases and in all cosmological eras, the presence of an effective w_{eff} which differs

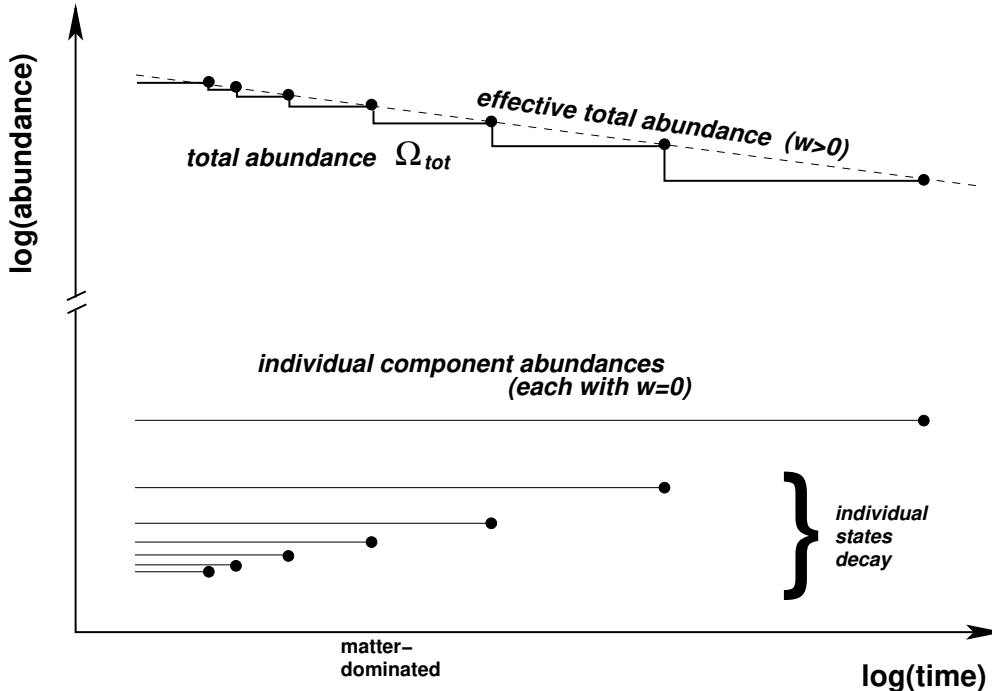


FIG. 2: A sketch of the total dark-matter abundance in our scenario during the final, matter-dominated era. Even though each dark-matter component individually has $w = 0$, the spectrum of lifetimes and abundances of these components conspire to produce a time-dependent total dark-matter abundance Ω_{tot} which corresponds to an effective equation of state with $w > 0$.

(however slightly) from zero would then signify a departure from the traditional dark-matter scenarios.

We can also understand this at a mathematical level. The fact that each individual dark-matter component has an abundance which follows the behavior in Eq. (1) with $w = 0$ does not guarantee that their *sum* Ω_{tot} must follow the same behavior. Indeed, the two effects which can alter the time-evolution of the sum Ω_{tot} in our scenario are a possible staggered turn-on at early times, and the individually decaying dark-matter components at late times. Thus the time-dependence of Ω_{tot} need not necessarily follow Eq. (1) with $w = 0$.

One possibility, of course, is that Ω_{tot} will continue to follow Eq. (1), but with some other effective value w_{eff} . However, even this outcome requires that our individual dark-matter components exhibit certain relationships between their abundances and lifetimes which need not actually hold for our dark-matter ensemble. Therefore, in general, we expect that Ω_{tot} might exhibit a time-dependence which does not resemble that given in Eq. (1) for *any* constant w_{eff} . Or, to phrase this somewhat differently, we expect that in general, our effective equation-of-state parameter w_{eff} might itself be time-dependent. We therefore seek to define a *function* $w_{\text{eff}}(t)$ which parametrizes a time-dependent equation of state for our dynamical dark-matter ensemble as a whole.

In order to define such an effective function $w_{\text{eff}}(t)$, let

us first recall that the traditional parameter w is fundamentally defined through the relation $p = w\rho$ where p and ρ are respectively the pressure and energy density of the “fluid” in question. Of course, in an FRW universe with radius R , the conservation law for energy density $dE = -pdV$ yields the relation $d(R^3\rho) = -pd(R^3)$, from which it immediately follows that $(p + \rho)dR^3/R^3 = -d\rho$ or $3(p + \rho)d\log R = -d\rho$. Recognizing $p + \rho = (1 + w)\rho$ and $d\log R = Hdt$ where H is the Hubble parameter, we thus have

$$3H(1 + w) = -\frac{d\log\rho}{dt}. \quad (6)$$

This is a completely general relation which makes no assumptions about the time-(in)dependence of w . We may therefore take this to be our fundamental definition for $w_{\text{eff}}(t)$ — *i.e.*,

$$\begin{aligned} w_{\text{eff}}(t) &\equiv -\left(\frac{1}{3H}\frac{d\log\rho_{\text{tot}}}{dt} + 1\right) \\ &= \begin{cases} -\frac{1}{2}\left(\frac{d\log\Omega_{\text{tot}}}{d\log t}\right) & \text{for RH/MD eras} \\ -\frac{2}{3}\left(\frac{d\log\Omega_{\text{tot}}}{d\log t}\right) + \frac{1}{3} & \text{for RD era} \end{cases} \end{aligned} \quad (7)$$

Note that while our derivation has thus far been com-

pletely general, we have specialized to specific cosmological eras in passing to the final expressions in Eq. (7). Specifically, we have written $\rho_{\text{tot}} = \Omega_{\text{tot}}\rho_{\text{crit}}$ and taken $3H \sim \kappa/t$ where $\kappa = 2$ (RH/MD), $\kappa = 3/2$ (RD).

The final expressions in Eq. (7) are easy to interpret physically, since the double-logarithmic derivatives which appear in these expressions are nothing but the slopes in the sketches in Figs. 1 and 2. However, the important point of this derivation has been to demonstrate that w_{eff} defined as in Eq. (7) continues to have a direct interpretation as a true equation-of-state parameter relating energy density and pressure, even when w_{eff} is time-dependent. No other definition of w_{eff} would have had this property.

The results in Eq. (7) provide a relation between w_{eff} and $\Omega_{\text{tot}}(t)$. However, it is also possible to derive a similar relation between w_{eff} and η . Assuming that we restrict our attention to periods of time *after* all staggered turn-ons are complete (so that the identity of the dark-matter component associated with Ω_0 is fixed), it trivially follows from the definition of η in Eq. (5) that

$$\frac{d \log(1 - \eta)}{d \log t} = \begin{cases} - \left(\frac{d \log \Omega_{\text{tot}}}{d \log t} \right) & \text{RH/MD eras} \\ - \left(\frac{d \log \Omega_{\text{tot}}}{d \log t} \right) + \frac{1}{2} & \text{RD era .} \end{cases} \quad (8)$$

Using the results in Eq. (7), we therefore find that

$$w_{\text{eff}}(t) = \begin{cases} \frac{1}{2} \left[\frac{d \log(1 - \eta)}{d \log t} \right] & \text{RH/MD eras} \\ \frac{2}{3} \left[\frac{d \log(1 - \eta)}{d \log t} \right] & \text{RD era .} \end{cases} \quad (9)$$

It therefore follows that decreasing η corresponds to positive w_{eff} , and vice versa. As a self-consistency check, we also observe that the standard paradigm — which has $\eta = 0$ for all times — has $w_{\text{eff}} = 0$ for all times as well.

2. Ω_{tot} , η , and w_{eff} : Qualitative time-dependent behaviors

Having defined the three quantities $\{\Omega_{\text{tot}}, \eta, w_{\text{eff}}\}$ that we will use in order to characterize a general configuration of our dark-matter ensemble, we now seek to understand the time-dependence that will be generically exhibited by these quantities across the different cosmological eras. As we shall see, several qualitative observations can be made even without further assumptions concerning the individual abundances and decay widths within our ensemble.

Given the sketch in Fig. 1, it is perhaps easiest to understand the qualitative behavior of Ω_{tot} as a function of time. There is, of course, the time-dependence for Ω_{tot} which can be associated with the regular Hubble expansion of the universe and which causes Ω_{tot} to increase during the radiation-dominated era. This aspect of the time-dependence is generally common to all dark-matter scenarios. However, as discussed above, there

are two additional effects which are specifically associated with our dynamical dark-matter scenario and which cause Ω_{tot} to experience a further time-dependence. The first of these is the possibility of a “staggered” turn-on across the different dark-matter components in our ensemble — *i.e.*, the possibility that some components will remain longer than others in a state in which their abundances Ω_i grow rapidly as $\sim t^2$ but contribute to the total *dark-energy* abundance rather than to Ω_{tot} . This feature, when present, will thus generally cause Ω_{tot} to experience a more gradual growth (but also a greater eventual maximum value) than would otherwise occur in a more traditional dark-matter scenario. However, at later stages of the cosmological evolution (particularly during the final, matter-dominated era), we see that our different dark-matter components have a broad spectrum of lifetimes and decay widths. This causes Ω_{tot} to experience a slow step-wise decline before finally reaching zero upon the decay of the last-surviving dark-matter component within the ensemble.

Similar qualitative arguments also apply to the time-evolution of η . An initial value of η is implicitly determined once the abundances for each of the dark-matter components are established. Of course, if this occurs during an inflationary period, it is possible that certain more massive components will have inflated away by the time the inflationary period ends. If this is the case, then we may regard the “initial” value of η to be the value of η at the end of the inflationary period.

In general, after that point, the evolution of η can experience as many as three distinct phases. Let t_1 denote the time at which the last (lightest) dark-matter component has turned on, and let t_2 denote the time at which the most massive dark-matter component decays. Assuming $t_2 > t_1$, there are therefore three distinct time intervals which become relevant.

During $t_1 \leq t \leq t_2$, each of the individual dark-matter abundances experiences a common overall time-dependent scaling behavior as the universe evolves. As a result, the ratio between the abundances of these components remains fixed. In other words, η remains frozen during this period (even though Ω_{tot} may continue to vary).

For $t > t_2$, by contrast, it is clear that the decays of the more massive dark-matter components have the cumulative effect of decreasing Ω_{tot} without altering Ω_0 . What results, then, is a step-by-step, threshold-by-threshold decline in the value of η . This process continues until only a single dark-matter component survives and η reaches zero. By assumption, in our scenario this will not happen until the distant future, at $t = \Gamma_1^{-1} \gg t_{\text{now}}$ where Γ_1 is the decay width of the second-lightest dark-matter component.

However, during the period $t < t_1$, a “staggered” turn-on for the individual dark-matter components can also generally induce a non-trivial time-evolution for η . Indeed, each time a new lightest dark-matter component turns on, its abundance Ω'_0 suddenly contributes to the

total dark-matter abundance Ω_{tot} . This abundance Ω'_0 also displaces the previous largest individual abundance Ω_0 . We therefore find that with each such successive turn-on, η experiences a shift in its value:

$$\eta \equiv 1 - \frac{\Omega_0}{\Omega_{\text{tot}}} \quad \longrightarrow \quad \eta' \equiv 1 - \frac{\Omega'_0}{\Omega_{\text{tot}} + \Omega'_0}. \quad (10)$$

By assumption, $\Omega'_0 > \Omega_0$. However, it is easy to see from Eq. (10) that $\eta' < \eta$ only if $\Omega'_0 > \Omega_0/\eta$. Since $0 \leq \eta \leq 1$, we see that this condition is guaranteed to be satisfied only if $\eta = 1$, and guaranteed *not* to be satisfied only if $\eta = 0$. In all other cases, this condition may or may not be satisfied, and this will cause η to either decrease or increase, respectively. We also observe that in a very rough sense, η tends to stabilize and avoid either the $\eta = 1$ or the $\eta = 0$ extremes: as $\eta \rightarrow 1$, it becomes easier and easier to satisfy the constraint that drives η lower, while as $\eta \rightarrow 0$, it becomes easier and easier to satisfy the constraint that pushes η higher. Indeed, if we imagine that each new abundance Ω'_0 somehow has a random value greater than the previous Ω_0 , we can envision an “oscillatory” behavior in which η varies between its two limits. Unfortunately, we cannot be more specific about this behavior without knowing something further about the individual abundances that exist during such a staggered turn-on phase.

We therefore conclude that η will take an initial value once the abundances are established, and that this value can then undergo a non-trivial time dependence if there is an initial period during which a staggered turn-on occurs. After the staggered turn-on is complete, η will remain frozen until late times when our individual dark-matter components begin to decay. This will then cause η to fall monotonically, ultimately vanishing when only the single longest-lived dark-matter component remains. However, it is regarded to be a fundamental property of our scenario that η is nevertheless presumed to be significantly different from zero at the present time.

Finally, we turn to the behavior of w_{eff} as a function of time. However, given the relations in Eq. (9), it is relatively straightforward to map out the rough time-dependence of w_{eff} . During the staggered turn-on phase (*i.e.*, $t < t_1$), we have seen that η may either increase or decrease; this implies that w_{eff} may be either negative or positive. Moreover, the fact that η tends to stabilize during this period, avoiding its extreme values at $\eta = 0$ or $\eta = 1$, implies that w_{eff} will likewise tend to stabilize around zero, with positive values of w_{eff} ultimately followed by negative values, and vice versa. As indicated above, however, this assumes that each new abundance Ω'_0 that turns on has a value which is greater than the previous Ω_0 but is otherwise somewhat random.

During the period $t_1 \leq t \leq t_2$, by contrast, the behavior of w_{eff} is far simpler to describe: we simply have $w_{\text{eff}} = 0$. This is completely in accord with our observation that η stays frozen during this period, and that our dynamical ensemble is behaving as ordinary dark-matter during this period (except with a non-zero value

of η). Finally, for the period $t > t_2$ after our individual dark-matter components have begun to decay, we have argued that η is monotonically decreasing. This implies that w_{eff} is strictly positive during this period, a feature which is illustrated in Fig. 2 and which again serves as a cosmological “smoking gun” for our dynamical dark-matter scenario.

D. A signature of dynamical dark matter: Time-evolution of Ω_{tot} , η , and w_{eff} during the final matter-dominated epoch

As just discussed, one of the most important signatures of our dynamical dark-matter framework is the fact that *the total dark-matter abundance Ω_{tot} is a time-evolving quantity — even during the current matter-dominated epoch.* Within such a framework, it is therefore only to be regarded as an accident that this quantity happens to reproduce a specific observed value $\Omega_{\text{CDM}} \approx 0.23$ at the present time.

With only a few additional assumptions, it turns out that we can explicitly calculate the time-evolution of the total dark-matter abundance Ω_{tot} during this epoch. We can also explicitly calculate the time-dependence of η , and the resulting equation of state $w_{\text{eff}}(t)$. In the rest of this section, we shall therefore concentrate on the final matter-dominated epoch. Indeed, this is the epoch during which a non-trivial time-evolution for Ω_{tot} arises only because of the decays of the individual dark-matter components within our ensemble.

Within this era, each dark matter component ϕ_i has a relative abundance Ω_i which remains constant until it decays at a time $t \sim \tau_i \equiv \Gamma_i^{-1}$. Taking this decay to be nearly instantaneous, we can thus write

$$\Omega_i(t) = \Omega_i \Theta(\tau_i - t), \quad (11)$$

whereupon we see that

$$\frac{d\Omega_{\text{tot}}(t)}{dt} = \sum_i \Omega_i \frac{d}{dt} \Theta(\tau_i - t) = - \sum_i \Omega_i \delta(\tau_i - t) \quad (12)$$

where we have defined $\Omega_{\text{tot}}(t) \equiv \sum_i \Omega_i(t)$ and used the relation $d\Theta(x)/dx = \delta(x)$ where $\delta(x)$ is the Dirac δ -function. In the limit that we truly have a large number of dark-matter states, we can imagine that the spectra of decay widths Γ_i and decay times $\tau_i \equiv \Gamma_i^{-1}$ are nearly continuous, with continuous variables Γ and τ . With this approximation, we can view Ω_i as a continuous function $\Omega(\tau)$ and convert the sum over states to an integral, *i.e.*,

$$\sum_i \implies \int d\tau n_\tau(\tau) \quad (13)$$

where $n_\tau(\tau)$ is the density of dark-matter states per unit of τ , expressed as a function of τ . Eq. (12) then becomes

$$\begin{aligned} \frac{d\Omega_{\text{tot}}(t)}{dt} &= - \int d\tau \Omega(\tau) n_\tau(\tau) \delta(\tau - t) \\ &= -\Omega(t) n_\tau(t). \end{aligned} \quad (14)$$

In general, the quantities $n(\tau)$ and $\Omega(\tau)$ are unspecified, their properties depending on the particular dark-matter scenario under study and the specific features of our dark-matter ensemble. However, it will prove convenient to parametrize these quantities in terms of their scaling behaviors as functions of Γ :

$$\Omega(\Gamma) \approx A\Gamma^\alpha, \quad n_\Gamma(\Gamma) \approx B\Gamma^\beta \quad (15)$$

with overall (generally dimensionful) coefficients (A, B) and scaling exponents (α, β) . Since the abundances of states in our scenario generally have an inverse relation to their decay widths, we expect that $\alpha < 0$. Note that n_Γ in Eq. (15) is the density of states per unit of Γ , whereupon it follows that

$$n_\tau = n_\Gamma \left| \frac{d\Gamma}{d\tau} \right| = \Gamma^2 n_\Gamma. \quad (16)$$

We thus find that $\Omega(\Gamma)n_\tau(\Gamma) \sim AB\Gamma^{\alpha+\beta+2}$, or equivalently $\Omega(\tau)n_\tau(\tau) \sim AB\tau^{-\alpha-\beta-2}$. Use of Eq. (14) then leads to the result

$$\frac{d\Omega_{\text{tot}}(t)}{dt} = -ABt^{-\alpha-\beta-2}. \quad (17)$$

Imposing the condition that $\Omega_{\text{tot}} = \Omega_{\text{CDM}}$ at the present time $t = t_{\text{now}}$ and assuming that $\alpha + \beta \neq -1$ then leads to the solution

$$\Omega_{\text{tot}}(t) = \Omega_{\text{CDM}} + \frac{AB}{\alpha + \beta + 1} (t^{-\alpha-\beta-1} - t_{\text{now}}^{-\alpha-\beta-1}). \quad (18)$$

For $\alpha + \beta = -1$, by contrast, we have the solution

$$\Omega_{\text{tot}}(t) = \Omega_{\text{CDM}} - AB \log\left(\frac{t}{t_{\text{now}}}\right). \quad (19)$$

Under the assumptions in Eq. (15), the results in Eqs. (18) and (19) are completely general in a matter-dominated era. Moreover, it is clear from Eqs. (18) and (19) that in all cases, Ω_{tot} decreases with time. This is precisely as expected, since all of the time dependence of Ω_{tot} in a matter-dominated era arises due to the decays of the individual dark-matter components within the ensemble. Notice that some of these functional forms for Ω_{tot} actually predict that $\Omega_{\text{tot}}(t)$ will eventually hit zero; this is also not unexpected, since this corresponds to the final decay of the last remaining dark-matter component in the ensemble. Needless to say, we should not consider any of these $\Omega_{\text{tot}}(t)$ functions beyond the times when they might hit zero. Nevertheless, as long as our dark-matter ensemble obeys the scaling laws in Eq. (15), the functions given in Eqs. (18) and (19) correctly describe the behavior of the corresponding total dark-matter abundances $\Omega_{\text{tot}}(t)$.

Given the results in Eqs. (18) and (19) as well as the definition in Eq. (7) for a matter-dominated era, we can also obtain a solution for the time-dependent equation-of-state parameter $w_{\text{eff}}(t)$ associated with our ensemble

of decaying dark-matter states. For $x \equiv \alpha + \beta \neq -1$, we find

$$w_{\text{eff}}(t) = \frac{(1+x)w_*}{2w_* + (1+x-2w_*)(t/t_{\text{now}})^{1+x}} \quad (20)$$

where

$$w_* \equiv w_{\text{eff}}(t_{\text{now}}) = \frac{AB}{2\Omega_{\text{CDM}}t_{\text{now}}^{1+x}}. \quad (21)$$

Note that for $w_* \ll 1$, this result is fairly well-approximated by

$$w_{\text{eff}}(t) \approx w_* \left(\frac{t}{t_{\text{now}}} \right)^{-x-1}. \quad (22)$$

By contrast, for $x = -1$, we instead obtain

$$w_{\text{eff}}(t) = \frac{w_*}{1 - 2w_* \log(t/t_{\text{now}})} \quad (23)$$

where

$$w_* \equiv w_{\text{eff}}(t_{\text{now}}) = \frac{AB}{2\Omega_{\text{CDM}}}. \quad (24)$$

The behavior of the results in Eqs. (20) and (23) depends critically on the relationship between x and w_* . For $1+x < 2w_*$, we find that w_{eff} always *increases* monotonically as a function of t before reaching w_* at $t = t_{\text{now}}$. By contrast, for $1+x > 2w_*$, this function *decreases* monotonically before reaching w_* at $t = t_{\text{now}}$. Finally, for $1+x = 2w_*$, we have the exact result that $w_{\text{eff}}(t) = w_*$ for all t . This (admittedly fine-tuned) case illustrates that it *is* possible to achieve a time-independent equation-of-state parameter $w_{\text{eff}} = w_*$ under the assumptions in Eq. (15), and moreover that this value of w_* can be tuned to any positive value desired. This is indeed the situation illustrated in Fig. 2, which is plotted for $\alpha < 0$ and $\beta > 0$.

The above qualitative descriptions indicate the history of $w_{\text{eff}}(t)$ prior to the present day. However, in general, this same increasing or decreasing behavior continues for $t > t_{\text{now}}$ (*i.e.*, through and beyond the current epoch), with one important caveat: for $1+x < 2w_*$, we see that $w_{\text{eff}}(t)$ not only continues to increase, but eventually hits a pole. However, such poles represent the locations at which the corresponding Ω_{tot} -functions have zeroes. These poles are therefore unphysical, signalling the decay of the last component within our dynamical dark-matter ensemble, and we can restrict our analysis of these functions to times preceding these critical values.

If our dynamical dark-matter scenario is to be in rough agreement with cosmological observations, we expect that w_* today should be fairly small (since traditional dark “matter” has $w = 0$). We also expect that the function $w_{\text{eff}}(t)$ should not have experienced strong variations within the recent past. This suggests that situations with $x < -1$ are likely to be phenomenologically preferred over those with $x \geq -1$, since having $x < -1$

ensures that $0 \leq w_{\text{eff}}(t) \leq w_*$ for all $t < t_{\text{now}}$. Indeed, the more negative x becomes, the closer to vanishing $w_{\text{eff}}(t)$ remains before finally reaching w_* at $t = t_{\text{now}}$. However, depending on the detailed properties of the particular realization of our dynamical dark-matter scenario under study, values of x near -1 or slightly above may also be phenomenologically acceptable.

Finally, we may also use these results to solve for η as a function of time. For $x \equiv \alpha + \beta \neq -1$, we find

$$\eta(t) = \frac{2w_* + [\eta_*(1+x) - 2w_*(t/t_{\text{now}})^{1+x}]}{2w_* + [1+x - 2w_*(t/t_{\text{now}})^{1+x}]} \quad (25)$$

where w_* is given in Eq. (21) and where

$$\eta_* \equiv \eta(t_{\text{now}}) = 1 - \frac{\Omega_0}{\Omega_{\text{CDM}}}. \quad (26)$$

Likewise, for $x = -1$, we have

$$\eta(t) = \frac{\eta_* - 2w_* \log(t/t_{\text{now}})}{1 - 2w_* \log(t/t_{\text{now}})} \quad (27)$$

where w_* is given in Eq. (24). It is not surprising that η , unlike w_{eff} , depends on *two* independent dimensionless quantities w_* and η_* , since the very definition for η introduces a new quantity Ω_0 which had not previously appeared.

Note that all time-dependence for $\eta(t)$ cancels, with $\eta(t) \approx \eta_*$ for all x , if either $w_* \rightarrow 0$ or $\eta_* \rightarrow 1$. This makes sense, since in the first case Ω_{tot} does not change while in the second case $\Omega_0 \rightarrow 0$. These are the only two ways in which η can remain constant. In all other cases, however, $\eta(t)$ is always a decreasing function of time, as expected. We also see from Eqs. (25) and (27) that $\eta(t) \rightarrow 1$ for all $x \geq -1$ as $t/t_{\text{now}} \rightarrow 0$. Indeed, this holds regardless of the values of w_* or η_* .

While these characteristics successfully conform to our expectations concerning the behavior of $\eta(t)$, there are some features that the functional forms in Eqs. (25) and (27) do not accurately capture. For example, if $x + 1 < 2w_*/\eta_*$, these functions predict that $\eta(t)$ will eventually become negative beyond a certain late time. Moreover, while these functions resemble those for w_{eff} in that they properly capture the pole that results when $\Omega_{\text{tot}} \rightarrow 0$, they do not necessarily approach $\eta \rightarrow 0$ before hitting this pole.

The reason behind these failures is easy to understand. Unlike Ω_{tot} and w_{eff} , the quantity η has a special characteristic not shared by the others: it is sensitive not only to Ω_{tot} , but also to Ω_0 . Features such as having η reach zero but not become negative are extremely sensitive to the value of Ω_0 and the fact that Ω_{tot} must exactly hit Ω_0 after all but the lightest dark-matter component have decayed. Indeed, these features are extremely sensitive to the fine-tuned and ultimately discrete nature of the lightest dark-matter components, and this is precisely the sort of information that our scaling assumptions in Eq. (15) are incapable of modelling. Thus, while we may view the

functions in Eqs. (25) and (27) as being reasonably accurate for most portions of the cosmological evolution in the matter-dominated era, we should not maintain this expectation beyond a certain time when all but a few dark-matter components have decayed.

To summarize, then, in this section we have presented a dynamical multi-component dark-matter scenario in which individual component abundances and lifetimes are balanced and distributed across the components in such a way that constraints from BBN and other backgrounds are potentially satisfied. An important part of this scenario is the proposition that both η and w_{eff} are different from zero at the present time, the former significantly so, and that components of the dark matter are actively decaying prior to, during, and beyond the current epoch. As a result, cosmological quantities such as Ω_{tot} experience a time-evolution which transcends that due to the ordinary expansion of the universe.

III. DYNAMICAL DARK MATTER MEETS THE INCREDIBLE BULK

Thus far, we have done little more than present a new framework for dark-matter physics. In particular, we have not yet demonstrated that an ensemble of dark-matter states can easily be assembled in which the individual component abundances are naturally balanced against lifetimes in a well-motivated way. In this section, however, we shall demonstrate that an infinite tower of Kaluza-Klein states propagating in the bulk of large extra spacetime dimensions naturally constitutes an ensemble of states with the desired properties. As we shall see, this occurs because KK towers obey a special “balancing” constraint which relates the lifetimes of individual KK modes to their abundances. Specifically, we shall demonstrate that the KK modes within a generic KK tower exhibit abundances Ω_i and SM decay widths Γ_i which obey an inverse relation of the form anticipated in Eq. (15), *i.e.*,

$$\Omega_i \Gamma_i^{-\alpha} \sim \text{constant} \quad (28)$$

for some $\alpha < 0$. This constraint ultimately emerges as a consequence of the non-trivial interplay between physics in the bulk and physics on the brane.

A. General setup

For simplicity, we shall consider our spacetime to take the form $\mathcal{M}_4 \times S_1/\mathbb{Z}_2$, where \mathcal{M}_4 denotes ordinary four-dimensional Minkowski spacetime and S_1/\mathbb{Z}_2 denotes a line segment which is realized as a \mathbb{Z}_2 orbifold of a circle of radius R . We shall take $z^M \equiv (x^\mu, y)$ to denote the coordinates on this spacetime, with the \mathbb{Z}_2 orbifold action identified as $y \rightarrow -y$, and imagine that the Standard Model is restricted to a brane at the fixed point $y = 0$. We are therefore considering a “toy” ADD-like

scenario [10] with a single flat extra dimension. Despite the simplicity of this toy model, we are making no assumptions at this stage about relevant mass scales or the full number of extra spacetime dimensions that might actually exist in a more fully realized scenario. Indeed, we believe that most of the desired properties that emerge from this scenario are likely to be retained if we imagine that our spacetime contains additional extra dimensions, or is warped [9] rather than flat.

In such a scenario, all fields that propagate in the “bulk” are necessarily singlets with respect to all Standard-Model gauge forces. As a result, such fields can have at most highly suppressed (*e.g.*, gravitational) interactions with the Standard-Model fields, and thus appear as dark-matter candidates. Such fields might include the graviton, axion, and other moduli fields. For simplicity, we shall consider the case in which the bulk field is a five-dimensional scalar Φ , but we shall make no further assumptions about its properties.

Neglecting gravity, and with ψ_i generically denoting the Standard-Model fields, we see that such a scenario therefore has an action of the form

$$S = \int d^4x dy [\mathcal{L}_{\text{bulk}}(\Phi) + \delta(y)\mathcal{L}_{\text{brane}}(\psi_i, \Phi)] . \quad (29)$$

In general, we may assume that our five-dimensional bulk action takes the form

$$\mathcal{L}_{\text{bulk}} = \frac{1}{2} \partial_M \Phi^* \partial^M \Phi - \frac{1}{2} M^2 |\Phi|^2 \quad (30)$$

where ∂_M denotes a five-dimensional derivative and where M is an unspecified bulk mass. In certain cases, specific symmetries may restrict us to the case with $M = 0$, but we shall leave M general until further notice.

Likewise, the brane action will generically consist of two contributions — the usual Standard-Model action \mathcal{L}_{SM} , and an action \mathcal{L}_{int} which arises due to the interactions between Φ and the Standard-Model fields:

$$\mathcal{L}_{\text{brane}} = \mathcal{L}_{\text{SM}} + \mathcal{L}_{\text{int}} . \quad (31)$$

In general, there are two types of interactions which will concern us. The first class of interactions result in explicit couplings between Φ and the Standard-Model fields, and will ultimately be responsible for allowing Φ to decay into Standard-Model states. We shall discuss such interactions in Sect. III.B. There is, however, another possible type of interaction term which can also appear within \mathcal{L}_{int} : this is a possible “brane mass” for Φ itself, *i.e.*,

$$\mathcal{L}_{\text{int}} \supset -\frac{1}{2} m^2 |\Phi|^2 . \quad (32)$$

Such a brane mass can emerge as an effective operator arising due to perturbative or non-perturbative dynamics wholly restricted to the brane. Note that this brane-mass term must not be confused with the primordial bulk mass that appears in Eq. (30); rather, this term has its origins within the physics on the brane itself, and appears as part of $\mathcal{L}_{\text{brane}}$ within Eq. (29) rather than $\mathcal{L}_{\text{bulk}}$.

These minimal assumptions are already sufficient to permit us to understand the nature of the resulting Kaluza-Klein spectrum for Φ . Indeed, the following results are similar to those previously obtained in Ref. [11]. As appropriate for compactification on the line segment S^1/\mathbb{Z}_2 , we can decompose our five-dimensional field Φ in terms of an infinite tower of four-dimensional modes ϕ_k ,

$$\Phi(x^\mu, y) = \frac{1}{\sqrt{2\pi R}} \sum_{k=0}^{\infty} r_k \phi_k(x^\mu) \cos\left(\frac{ky}{R}\right) ; \quad (33)$$

the normalization factors

$$r_k \equiv \begin{cases} 1 & \text{for } k = 0 \\ \sqrt{2} & \text{for } k > 0 \end{cases} \quad (34)$$

are designed to ensure that each mode ϕ_k has a canonically normalized kinetic term in the resulting four-dimensional theory. We then find that

$$\begin{aligned} S &= \int d^4x dy \left[\frac{1}{2} \partial_M \Phi^* \partial^M \Phi - \frac{1}{2} M^2 |\Phi|^2 - \frac{1}{2} \delta(y) m^2 \Phi^2 \right] \\ &= \int d^4x \left(\frac{1}{2} \sum_{k=0}^{\infty} \partial_\mu \phi_k^* \partial^\mu \phi_k - \frac{1}{2} \sum_{k,\ell=0}^{\infty} \mathcal{M}_{k\ell}^2 \phi_k \phi_\ell^* \right) \end{aligned} \quad (35)$$

where the Kaluza-Klein (mass)² matrix is given by

$$\mathcal{M}_{k\ell}^2 = \left(\frac{k\ell}{R^2} + M^2 \right) \delta_{k\ell} + r_k r_\ell m^2 . \quad (36)$$

Given these results, we see that this mass matrix would have been diagonal were it not for the brane mass term. This in turn implies that the KK mass eigenstates ϕ_λ necessarily differ from the KK momentum eigenstates ϕ_k — *i.e.*, there is a non-trivial *mixing* that is induced as a result of the KK mass. This mixing turns out to be critical for our analysis. In general, we may characterize the degree of mixing in terms of the dimensionless parameter

$$y \equiv \frac{1}{mR} . \quad (37)$$

For $y \gg 1$ the mass matrix is essentially diagonal; this is what trivially occurs, for example, in the four-dimensional $R \rightarrow 0$ limit in which the excited KK modes decouple. By contrast, in the opposite limit $y \ll 1$, the mixing is essentially maximal across all of the eigenmodes.

It is possible to describe the solutions for the eigenvalues λ^2 of the (mass)² matrix in closed form, and thereby obtain explicit expressions for the corresponding mass eigenstates. The eigenvalues turn out to be the solutions to the transcendental equation

$$\pi m^2 R \cot\left(\pi R \sqrt{\lambda^2 - M^2}\right) = \sqrt{\lambda^2 - M^2} . \quad (38)$$

If m were zero (*i.e.*, no brane mass), the solutions to this equation would be nothing but the expected eigenvalues

$$\lambda_n^2 = M^2 + \frac{n^2}{R^2} , \quad n \in \mathbb{Z} , \quad (39)$$

and more generally this remains approximately true when $m \ll 1/R$, *i.e.*, when $y \gg 1$. What is perhaps surprising, however, is that the presence of a non-zero brane mass does not result in a further additive shift in this mass spectrum for the KK tower (as does the bulk mass term), but instead distorts the lower mass eigenstates in the tower so that they approximately follow the alternate spectrum

$$\lambda_n^2 = M^2 + \frac{(n + \frac{1}{2})^2}{R^2}, \quad n \in \mathbb{Z}. \quad (40)$$

Remarkably, this is precisely the spectrum which we would normally associate with a five-dimensional field Φ which is taken to be *anti-periodic* (rather than periodic) around the extra-dimensional circle prior to orbifolding! Indeed, for general values of y , the solutions λ_n of Eq. (38) tend to follow the spectrum in Eq. (40) for $n \ll \pi/y^2$, while they follow the spectrum in Eq. (39) for $n \gg \pi/y^2$ and smoothly transition between the two spectra for intermediate values $n \sim \pi/y^2$. As we have discussed above, this unusual behavior is the consequence of the non-trivial interplay between brane and bulk physics, and may have applications beyond its appearance here.

For each mass eigenvalue λ , we can also solve for the corresponding mass eigenstate $|\phi_\lambda\rangle$ as a linear combination of the KK-momentum eigenstates $|\phi_k\rangle$. We find the exact result [11]

$$|\phi_\lambda\rangle = A_\lambda \sum_{k=0}^{\infty} \frac{r_k \tilde{\lambda}^2}{\tilde{\lambda}^2 - k^2 y^2} |\phi_k\rangle \quad (41)$$

where we have defined the dimensionless eigenvalues

$$\tilde{\lambda} \equiv \sqrt{\lambda^2 - M^2}/m \quad (42)$$

and where

$$A_\lambda \equiv \frac{\sqrt{2}}{\tilde{\lambda}} \frac{1}{\sqrt{1 + \pi^2/y^2 + \tilde{\lambda}^2}}. \quad (43)$$

Given these results, it is straightforward to convert between the mass-eigenstate basis $|\phi_\lambda\rangle$ and the KK-momentum basis $|\phi_k\rangle$. It turns out that there are two specific groups of matrix elements involved in this conversion which will be of particular interest to us. The first involves the KK zero-mode $\phi_{k=0}$, for which we have the matrix elements

$$\langle \phi_\lambda | \phi_{k=0} \rangle = A_\lambda. \quad (44)$$

However, the second concerns the *projection* of the five-dimensional bulk field $\Phi(y)$ onto the Standard-Model brane at $y = 0$, *i.e.*,

$$\phi' \equiv \Phi(y)|_{y=0} = \sum_{k=0}^{\infty} r_k \phi_k. \quad (45)$$

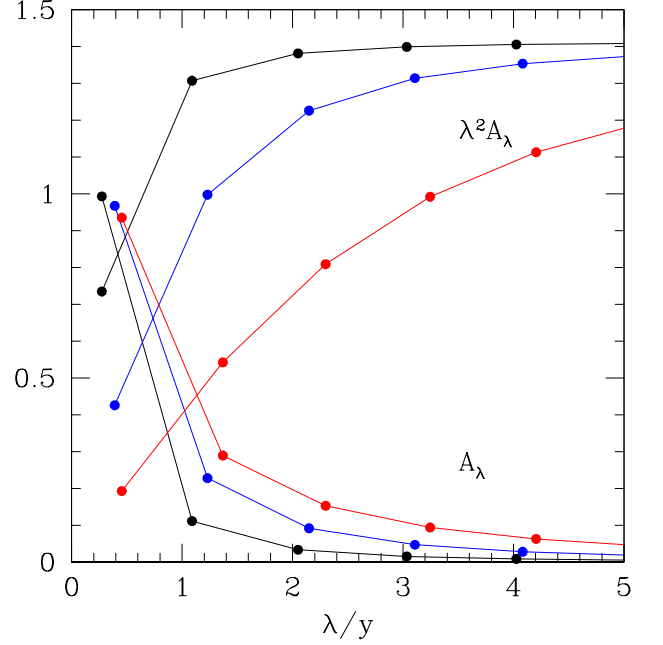


FIG. 3: Values of A_λ (falling curves) and $\tilde{\lambda}^2 A_\lambda$ (rising curves), plotted as functions of the mass eigenvalues $\tilde{\lambda}/y = \lambda R$ for $y = \pi$ (black), $y = \sqrt{\pi}$ (blue), and $y = 1$ (red). For each y , there are only a discrete set of corresponding allowed eigenvalues $\tilde{\lambda}$ (indicated with solid dots); note that the quantity $\tilde{\lambda}/y = \sqrt{\lambda^2 - M^2}R$ takes values closer to $\mathbb{Z} + 1/2$ near the bottom of each tower and shifts to values closer to \mathbb{Z} as λ increases. In each case, we see that A_λ falls with increasing $\tilde{\lambda}$, while $\tilde{\lambda}^2 A_\lambda$ increases with increasing $\tilde{\lambda}$ and ultimately reaches an asymptote $\tilde{\lambda}^2 A_\lambda \rightarrow \sqrt{2}$ as $\tilde{\lambda} \rightarrow \infty$.

For this projection field, we likewise have the matrix elements

$$\begin{aligned} \langle \phi_\lambda | \phi' \rangle &= A_\lambda \sum_{k=0}^{\infty} \frac{r_k^2 \tilde{\lambda}^2}{\tilde{\lambda}^2 - k^2 y^2} \\ &= \frac{\pi \tilde{\lambda}^2}{y} \cot\left(\frac{\pi \tilde{\lambda}}{y}\right) A_\lambda = \tilde{\lambda}^2 A_\lambda \end{aligned} \quad (46)$$

where we have made use of Eq. (38) in the final equality.

In Fig. 3, we plot the values of A_λ and $\tilde{\lambda}^2 A_\lambda$ as functions of $\tilde{\lambda}$ and y . We see that A_λ falls with increasing $\tilde{\lambda}$, while $\tilde{\lambda}^2 A_\lambda$ increases with increasing $\tilde{\lambda}$ and ultimately reaches an asymptote $\tilde{\lambda}^2 A_\lambda \rightarrow \sqrt{2}$ as $\tilde{\lambda} \rightarrow \infty$. Moreover, we see that larger and larger values of λ are needed to reach this asymptote as y decreases.

B. Balancing Γ versus Ω

We now address the central feature underpinning dynamical dark matter: the balance between the SM decay widths Γ_λ associated with each KK mass eigenstate and the corresponding cosmological abundances Ω_λ . As we

shall show, an inverse relation of the form anticipated in Eq. (28) naturally emerges across the entire KK tower.

1. Abundances Ω_λ

We begin by focusing on the different cosmological mode abundances Ω_λ that can arise in such a scenario.

During the course of the evolution of the universe, there are many production mechanisms through which the different KK states might come to be populated and thereby acquire non-zero abundances. One such method, for example, is thermal production; another relies on purely geometric effects (*e.g.*, topological defects such as cosmic strings and domain walls) and the decays associated with them. However, there is also a third production mechanism which exists in cases where the bulk mass M happens to vanish: this is so-called “misalignment production”.

In many string-theoretic contexts, bulk fields often do have vanishing bulk masses. Such fields often include gravitational and/or geometric moduli fields; they also include various axion-like fields. Moreover, as we shall demonstrate, the predictions of misalignment production are rather straightforward to calculate, and are fairly generic for bulk fields as a whole. We shall therefore take $M = 0$ in what follows, and restrict our attention to abundances established through misalignment production.

It is easy to understand the physical underpinnings of misalignment production within the framework of dynamical dark matter. Prior to the brane dynamics that establishes the brane mass m , the fact that $M = 0$ implies that our theory exhibits a five-dimensional shift symmetry $\Phi \rightarrow \Phi + c$, where c is a constant. As a result, any value for $\langle \Phi \rangle$ is equally likely to occur:

$$\langle \Phi \rangle = \theta f_\Phi^{3/2} \quad (47)$$

where θ is a random $\mathcal{O}(1)$ dimensionless coefficient and where f_Φ is a mass scale (or decay constant) associated with the five-dimensional Φ field in the bulk. Decomposed into KK eigenstates via Eq. (33), this non-zero vev for the five-dimensional field Φ implies a non-zero vev for the KK zero mode:

$$\langle \phi_0 \rangle = \theta \hat{f}_\phi, \quad \langle \phi_k \rangle = 0 \quad \text{for all } k > 0 \quad (48)$$

where

$$\hat{f}_\phi \equiv \sqrt{2\pi R} f_\Phi^{3/2}. \quad (49)$$

Note that all of the higher KK modes ϕ_k with $k > 0$ must have vanishing vevs as a result of the five-dimensional shift symmetry.

This is the situation that exists prior to (*i.e.*, at energies higher than those associated with) the brane dynamics that establishes the brane mass m . However, once

this brane mass is established, we must shift to the *mass-eigenstate* basis, whereupon we see from Eq. (44) that Eq. (48) now takes the form

$$\langle \phi_\lambda \rangle = \theta A_\lambda \hat{f}_\phi \quad \text{for all } \lambda. \quad (50)$$

Thus, we see that *all* of the mass eigenstates will generally have non-zero values. Of course, the fact that these vevs are all related through the coefficients A_λ is a reflection of our original five-dimensional shift symmetry in the bulk.

The dynamics that establishes the brane mass m also leads to a non-zero energy density ρ associated with the configuration in Eq. (50). In general, the four-dimensional energy density ρ_λ associated with each mode ϕ_λ is given by $\rho_\lambda = \frac{1}{2}\lambda^2 \langle \phi_\lambda \rangle^2$. Given Eq. (50), we thus have

$$\rho_\lambda = \frac{1}{2}\theta^2 \lambda^2 A_\lambda^2 \hat{f}_\phi^2. \quad (51)$$

Of course, at any moment in the evolution of the universe, the *critical* energy density is given by

$$\rho_{\text{crit}} = 3M_P^2 H^2 \quad (52)$$

where $M_P \equiv (8\pi G_N)^{-1/2}$ is the *reduced* Planck scale and where H is the Hubble parameter. The initial abundance $\Omega_\lambda \equiv \rho_\lambda / \rho_{\text{crit}}$ associated with the ϕ_λ mode is thus given by

$$\Omega_\lambda^{(0)} = \frac{\theta^2}{6} \tilde{\lambda}^2 A_\lambda^2 \left(\frac{m \hat{f}_\phi}{M_P H} \right)^2. \quad (53)$$

This is, in fact, a completely general result.

We shall let t_0 denote the time at which this initial abundance is established by the brane dynamics. Thus $\Omega_\lambda(t_0) = \Omega_\lambda^{(0)}$. The next question, however, is to determine the corresponding value of $\Omega_\lambda(t_{\text{now}})$. In order to do this, we see from Fig. 1 that we must make some assumptions about whether t_0 is situated during the reheating, radiation-dominated, or matter-dominated eras, and whether the ϕ_λ mode experiences an instantaneous turn-on at t_0 or a staggered turn-on at a time $t_\lambda > t_0$. There are therefore six different cases to consider.

For simplicity we shall assume that for the modes ϕ_λ which are part of a staggered turn-on, the corresponding turn-on time t_λ occurs at the threshold $3H(t_\lambda) = 2\lambda$. (Of course, if $t_\lambda \leq t_0$, then such modes turn on only at t_0 .) We shall also assume that all modes in a given tower actually turn on during the same era as t_0 , so that our turn-on “cascade” down the tower does not cross a boundary between two different eras. Finally, we shall assume that within each era, $H(t)$ takes the approximate form $H(t) = \kappa/3t$ where $\kappa = 2$ for the reheating and matter-dominated eras and $\kappa = 3/2$ during the radiation-dominated era. This implies that $t_\lambda = \kappa/2\lambda$. Note that this approximate form for $H(t)$ is generally valid at relatively late times within each era, and we shall disregard all $\mathcal{O}(1)$ “threshold” effects associated

with the boundaries between different eras. Thus, we shall implicitly take Ω_λ to be a continuous function of t , as sketched in Fig. 1, and we shall therefore disregard all $\tilde{\lambda}$ -independent $\mathcal{O}(1)$ numerical coefficients in those expressions for $\Omega_\lambda(t_{\text{now}})$ which follow.

Clearly, if t_0 occurs during the final matter-dominated era (*i.e.*, if $t_0 > t_{\text{MRE}}$), then modes which turn on instantaneously (*i.e.*, modes with $t_\lambda \leq t_0$) will have abundances

$$\Omega_\lambda(t_{\text{now}}) \sim X_\lambda \Omega_\lambda^{(0)} \sim \tilde{\lambda}^2 A_\lambda^2 X_\lambda \left(\frac{\hat{f}_\phi}{M_P} \right)^2 (mt_0)^2 \quad (54)$$

where X_λ denotes the expected damping factor due to dark-matter decays:

$$X_\lambda \equiv e^{-\Gamma_\lambda(t_{\text{now}}-t_0)}. \quad (55)$$

By contrast, for those modes which experience a staggered turn-on (*i.e.*, modes with $t_\lambda > t_0$), this result becomes

$$\Omega_\lambda(t_{\text{now}}) \sim X_\lambda \Omega_\lambda^{(0)} \left(\frac{t_\lambda}{t_0} \right)^2 \sim A_\lambda^2 X_\lambda \left(\frac{\hat{f}_\phi}{M_P} \right)^2 \quad (56)$$

where we have substituted the result $t_\lambda \sim 1/\lambda$ in passing to the final expression.

By contrast, for t_0 within the radiation-dominated era (*i.e.*, $t_{\text{RH}} \lesssim t_0 \lesssim t_{\text{MRE}}$), these two cases are instead given by

$$\begin{aligned} \Omega_\lambda(t_{\text{now}}) &\sim X_\lambda \Omega_\lambda^{(0)} \left(\frac{t_{\text{MRE}}}{t_0} \right)^{1/2} \\ &\sim \tilde{\lambda}^2 A_\lambda^2 X_\lambda \left(\frac{\hat{f}_\phi}{M_P} \right)^2 (mt_0)^{3/2} (mt_{\text{MRE}})^{1/2} \end{aligned} \quad (57)$$

and

$$\begin{aligned} \Omega_\lambda(t_{\text{now}}) &\sim X_\lambda \Omega_\lambda^{(0)} \left(\frac{t_\lambda}{t_0} \right)^2 \left(\frac{t_{\text{MRE}}}{t_\lambda} \right)^{1/2} \\ &\sim \tilde{\lambda}^{1/2} A_\lambda^2 X_\lambda \left(\frac{\hat{f}_\phi}{M_P} \right)^2 (mt_{\text{MRE}})^{1/2}. \end{aligned} \quad (58)$$

Finally, for t_0 within the reheating era (*i.e.*, $t_0 \lesssim t_{\text{RH}}$), these two cases are instead given by

$$\begin{aligned} \Omega_\lambda(t_{\text{now}}) &\sim X_\lambda \Omega_\lambda^{(0)} \left(\frac{t_{\text{MRE}}}{t_{\text{RH}}} \right)^{1/2} \\ &\sim \tilde{\lambda}^2 A_\lambda^2 X_\lambda \left(\frac{\hat{f}_\phi}{M_P} \right)^2 (mt_0)^2 \left(\frac{t_{\text{MRE}}}{t_{\text{RH}}} \right)^{1/2} \end{aligned} \quad (59)$$

and

$$\begin{aligned} \Omega_\lambda(t_{\text{now}}) &\sim X_\lambda \Omega_\lambda^{(0)} \left(\frac{t_\lambda}{t_0} \right)^2 \left(\frac{t_{\text{MRE}}}{t_{\text{RH}}} \right)^{1/2} \\ &\sim A_\lambda^2 X_\lambda \left(\frac{\hat{f}_\phi}{M_P} \right)^2 \left(\frac{t_{\text{MRE}}}{t_{\text{RH}}} \right)^{1/2}. \end{aligned} \quad (60)$$

Interestingly, of all six cases, this is the only one which yields a result for $\Omega_\lambda(t_{\text{now}})$ which is parametrically independent of the scale m .

It is also instructive to examine the manner in which these results scale with $\tilde{\lambda}$. Surveying Eqs. (54) through (60), we see that the dependence of Ω_λ on $\tilde{\lambda}$ follows only three different patterns, depending on the specific turn-on behavior experienced by the KK mode in question and the era during which it takes place:

$$\Omega_\lambda \sim \begin{cases} \tilde{\lambda}^2 A_\lambda^2 & \text{instantaneous} \\ \tilde{\lambda}^{1/2} A_\lambda^2 & \text{staggered (RD era)} \\ A_\lambda^2 & \text{staggered (RH/MD eras)}. \end{cases} \quad (61)$$

Under the assumption of misalignment production, this result is exact and completely general. However, given the definition in Eq. (43), we may approximate

$$A_\lambda \sim \begin{cases} 1/\tilde{\lambda} & \text{for } \tilde{\lambda} \ll \sqrt{1 + \pi^2/y^2} \\ 1/\tilde{\lambda}^2 & \text{for } \tilde{\lambda} \gg \sqrt{1 + \pi^2/y^2}. \end{cases} \quad (62)$$

In the future, we shall refer to these two approximation regimes as the small- $\tilde{\lambda}$ and large- $\tilde{\lambda}$ regimes; note that while there always exists a large- $\tilde{\lambda}$ regime, the existence of a small- $\tilde{\lambda}$ regime depends on the value of y . We then find that the results in Eq. (61) lead to the large- $\tilde{\lambda}$ scaling behaviors

$$\Omega_\lambda \sim \begin{cases} \tilde{\lambda}^{-2} & \text{instantaneous} \\ \tilde{\lambda}^{-7/2} & \text{staggered (RD era)} \\ \tilde{\lambda}^{-4} & \text{staggered (RH/MD eras)} \end{cases} \quad (63)$$

as well as the small- $\tilde{\lambda}$ behaviors

$$\Omega_\lambda \sim \begin{cases} \text{constant} & \text{instantaneous} \\ \tilde{\lambda}^{-3/2} & \text{staggered (RD era)} \\ \tilde{\lambda}^{-2} & \text{staggered (RH/MD eras)}. \end{cases} \quad (64)$$

Indeed, the only λ -dependence which is not included in these results is that which appears through the decay widths in the X_λ -factors in Eqs. (54) through (60). However, these X_λ factors only express the physics of the eventual dark-matter *decay* processes; they play no role in determining the mode abundances that exist *prior* to decay, which is our main interest in this discussion. As a result, we shall disregard these X_λ factors in what follows, understanding that our analysis is primarily appropriate for the period that exists *prior* to the onset of decays of the KK states with significant abundances. (Indeed, the final period of KK decays will be discussed

in Sect. III.B.3 after we have analyzed the behavior of the decay widths Γ_λ in Sect. III.B.2.)

Given the individual abundances Ω_λ in Eqs. (54) through (60), we can now calculate the values of both Ω_{tot} and η that exist prior to the onset of significant KK decays. Recall that Ω_{tot} is nothing but the sum over all of the individual abundances Ω_λ , while η describes how that total abundance is distributed across the different modes. Indeed, we see from Eq. (63) that the lightest of the KK modes will always carry the greatest abundance. It then follows from its definition in Eq. (5) that η indicates what fraction of the total abundance is carried by the *excited* states in the KK tower. For this reason we shall occasionally refer to η as the “tower fraction”.

Let us first consider Ω_{tot} . At first glance, it might seem algebraically cumbersome to tally these individual mode abundances Ω_λ , since they each have a different λ -dependence given in Eq. (61) and we would need to sum over all of the eigenvalue solutions to the transcendental equation in Eq. (38). However, it turns out that the resulting spectrum of λ -eigenvalues satisfies two critical identities [11]:

$$\sum_\lambda A_\lambda^2 = 1, \quad \sum_\lambda \tilde{\lambda}^2 A_\lambda^2 = 1. \quad (65)$$

These identities ultimately stem from the unitary nature of the mapping between the KK-momentum basis and the mass-eigenstate basis. Thus, unless our KK tower experiences a staggered turn-on during the radiation-dominated era, summing over the individual abundances in Eq. (61) is particularly simple.

What is truly remarkable about the identities in Eq. (65) is that they hold for all values of y . They are thus independent of the degree of non-diagonality exhibited by the KK mass matrix, and independent of the degree to which the corresponding KK modes are mixed. As a result, if we assume that \hat{f}_ϕ , t_0 , and m are all y -independent, it then follows that Ω_{tot} will be y -independent as well! Although dialing the value of y (*i.e.*, adjusting the radius of the extra spacetime dimension) might change the *distribution* of abundances across the infinite tower of KK states, the *total* abundance remains essentially fixed.

We stress that this result holds only for those cases in which the KK abundances are established either instantaneously, or through a staggered turn-on which takes place during the reheating or matter-dominated eras. By contrast, if these KK abundances are established through a staggered turn-on during the *radiation*-dominated era, the total abundance Ω_{tot} today will be proportional to $\sum_\lambda \tilde{\lambda}^{1/2} A_\lambda^2$. This quantity is not y -independent, but rather has the y -dependence shown in Fig. 4. As a result, our preferred choices for parametric quantities such as \hat{f}_ϕ , t_0 , and m would need to be altered in order to compensate for this effect.

The results in Eq. (61) also allow us to calculate the tower fraction η prior to the onset of significant KK decays. Indeed, the three different patterns for Ω_λ in

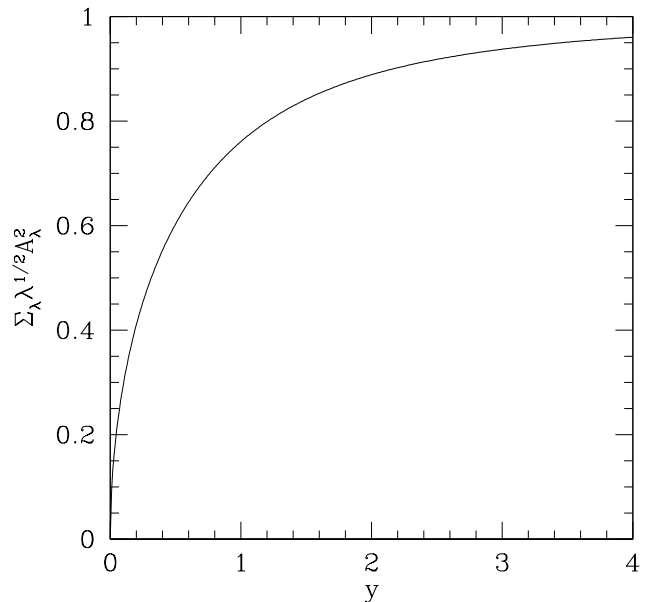


FIG. 4: The quantity $\sum_\lambda \tilde{\lambda}^{1/2} A_\lambda^2$, plotted as a function of y . Note that the total dark-matter abundance Ω_{tot} prior to the onset of significant KK decays is proportional to this quantity if the individual KK abundances are initially established through a staggered turn-on during the radiation-dominated era. As a result, this curve also illustrates the y -dependence of Ω_{tot} in this case. By contrast, for all other cases, the total abundance Ω_{tot} is y -independent.

Eq. (61) imply three different distributions for the abundances across the different mass eigenstates in the KK tower. Therefore, if we additionally assume that all of the states in a given tower simultaneously fall into one of these three cases, there will be three corresponding possible behaviors for the “tower fraction” η defined in Eq. (5), viewed as a function of the non-diagonality parameter y . These results are shown in Fig. 5, and we see that η indeed spans a range of $\mathcal{O}(1)$ values, as desired. These results are also highly y -dependent, illustrating that while adjusting y changes the total abundance only in certain restricted circumstances, it changes the *distribution* of these abundances quite substantially in all cases.

It is easy to understand the overall features exhibited in Fig. 5. As $y \rightarrow \infty$, we enter the four-dimensional limit in which virtually no abundance is carried by the excited KK modes. As a result, these modes become completely irrelevant to the dark-matter problem, and $\eta \rightarrow 0$. By contrast, as $y \rightarrow 0$, our KK states experience maximal mixing, as a result of which the corresponding value of η is maximized. Since $\lambda_n \approx (n + \frac{1}{2})/R$ for all n in this limit, we can easily calculate these maximum values of η , obtaining the result that $\eta_{\text{max}} = 1$ in the case of instantaneous turn-on, while for the case of staggered turn-on during a reheating or matter-dominated era we

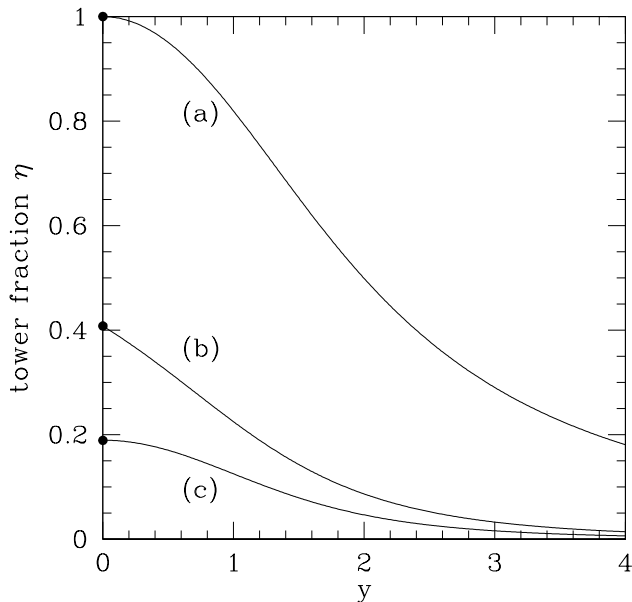


FIG. 5: The tower fraction η after all dark-matter modes have “turned on” and entered the present matter-dominated epoch, plotted as a function of y for three different regimes of misalignment production: (a) instantaneous turn-on, in which case $\Omega_\lambda \sim \tilde{\lambda}^2 A_\lambda^2$; (b) staggered turn-on during a radiation-dominated era, in which case $\Omega_\lambda \sim \tilde{\lambda}^{1/2} A_\lambda^2$; and (c) staggered turn-on during a reheating or matter-dominated era, in which case $\Omega_\lambda \sim A_\lambda^2$. In each case we see that $\eta \rightarrow 0$ as $y \rightarrow \infty$, while η approaches a fixed maximum value η_{\max} as $y \rightarrow 0$.

have

$$\begin{aligned} \eta_{\max} &= 1 - 4 \left[\sum_{n=0}^{\infty} \frac{1}{(n+1/2)^2} \right]^{-1} \\ &= 1 - \frac{8}{\pi^2} \approx 0.189, \end{aligned} \quad (66)$$

and for the case of staggered turn-on during a radiation-dominated era we have

$$\begin{aligned} \eta_{\max} &= 1 - 2\sqrt{2} \left[\sum_{n=0}^{\infty} \frac{1}{(n+1/2)^{3/2}} \right]^{-1} \\ &= 1 - \frac{2\sqrt{2}}{(2\sqrt{2}-1)\zeta(3/2)} \approx 0.408 \end{aligned} \quad (67)$$

where ζ denotes the Riemann zeta-function. All three of these limiting values are evident in Fig. 5.

2. Decay widths Γ_λ

Next, we turn to the decay widths Γ_λ which can be expected in such a scenario.

Up to this point, we have assumed nothing more than that the bulk field in our setup has a vanishing bulk mass

$M = 0$ and a non-vanishing brane mass $m \neq 0$. As we have seen, this has proven sufficient to allow us to determine not only the Kaluza-Klein “spectroscopy” of our dark towers but also the corresponding cosmological mode abundances that emerge from misalignment production. In some sense, it is remarkable that these results rely on such minimal assumptions; indeed, this happy fact explains why our results thus far are extremely general and can be expected to hold for all bulk fields for which $M = 0$ and $m \neq 0$.

However, in order to discuss the decay widths of these KK modes into Standard-Model states, we shall require further information concerning the couplings between the five-dimensional bulk field Φ and the four-dimensional Standard-Model states. In other words, we shall require further information concerning the interaction terms that might appear within \mathcal{L}_{int} in Eq. (31) and thereby become part of our four-dimensional effective Lagrangian. Of course, it is most dangerous for the consistency and phenomenological viability of our dynamical dark-matter scenario if these decay widths are too large. Our conservative approach to this problem will therefore be to consider the worst possible scenario and determine how large these decay widths might be. Since the largest decay widths will generally arise from the operators of lowest possible dimension within \mathcal{L}_{int} , the first step in our analysis is therefore to determine what forms such operators might take.

Imposing Lorentz invariance and invariance under all Standard-Model gauge symmetries, we find that our options are fairly limited. The separate brane/bulk structure of this dark-matter setup requires that our bulk dark-matter field Φ be a singlet under all Standard-Model gauge symmetries. This implies that any combinations of brane fields to which Φ couples must be gauge invariant by themselves. Moreover, in order to restrict ourselves to operators of lowest possible dimensionality, we shall consider operators which are at most linear in Φ . We shall also assume for this discussion that Φ is real. Letting ψ denote a generic Standard-Model fermion and $F_{\mu\nu}$ denote a generic Standard-Model field strength for any gauge group, we then find that the operators of lowest possible dimensionality come in two groups. If Φ is CP-even, the lowest-dimension operators which may appear in \mathcal{L}_{int} take the form

$$\frac{1}{f_\Phi^{3/2}} \Phi \bar{\psi} \gamma^\mu \partial_\mu \psi, \quad \frac{1}{f_\Phi^{3/2}} \Phi F_{\mu\nu} F^{\mu\nu} \quad (68)$$

where f_Φ is the five-dimensional mass scale associated with Φ which originally appeared in Eq. (47). By contrast, if Φ is CP-odd, the lowest-dimension operators which may appear in \mathcal{L}_{int} take the form

$$\frac{1}{f_\Phi^{3/2}} (\partial_\mu \Phi) \bar{\psi} \gamma^\mu \gamma^5 \psi, \quad \frac{1}{f_\Phi^{3/2}} \Phi F_{\mu\nu} \tilde{F}^{\mu\nu} \quad (69)$$

where $\tilde{F}^{\mu\nu} \sim \epsilon^{\mu\nu\rho\sigma} F_{\rho\sigma}$. These groups of operators then

respectively give rise to the four-dimensional couplings

$$\frac{1}{\hat{f}_\phi} \phi' \bar{\psi} \gamma^\mu \partial_\mu \psi, \quad \frac{1}{\hat{f}_\phi} \phi' F_{\mu\nu} F^{\mu\nu} \quad (70)$$

and

$$\frac{1}{\hat{f}_\phi} (\partial_\mu \phi') \bar{\psi} \gamma^\mu \gamma^5 \psi, \quad \frac{1}{\hat{f}_\phi} \phi' F_{\mu\nu} \tilde{F}^{\mu\nu} \quad (71)$$

where ϕ' , as defined in Eq. (45), is the projection of Φ onto the Standard-Model brane, and where \hat{f}_ϕ is defined in Eq. (49).

This list exhausts the possible dimension-five operators. It is encouraging that we see among this list of possible operators the standard moduli and axion couplings — indeed, in the CP-even case we can even regard the linear prefactor ϕ'/\hat{f}_ϕ as the leading term of an exponential prefactor $\exp(\phi'/\hat{f}_\phi)$, and thereby recognize the standard dilaton coupling in string theory. Thus, this list of operators includes most of our cases of phenomenological interest. At first glance, it might seem that operators of even lower dimension could be constructed — *e.g.*, $\Phi \bar{\psi} \psi$ and $\Phi \bar{\psi} \gamma^5 \psi$. However, such operators are not gauge invariant because all of the fermions ψ in the Standard Model are chiral. Likewise, dimension-four operators such as $|\Phi|^2 |H|^2$ are also forbidden as they would violate the shift symmetry under which $\Phi \rightarrow \Phi + \text{constant}$.

Although kinematic effects favor the di-photon decay mode $\phi' \rightarrow \gamma\gamma$, the four-dimensional couplings in Eqs. (70) and (71) all lead to SM decay rates of the same parametric order. Standard calculations then lead to an overall decay width

$$\Gamma_\lambda \sim \frac{\lambda^3}{\hat{f}_\phi^2} \langle \phi_\lambda | \phi' \rangle^2 = \frac{\lambda^3}{\hat{f}_\phi^2} (\tilde{\lambda}^2 A_\lambda)^2 \quad (72)$$

where we have substituted Eq. (46) in the final step. Use of Eqs. (62) then leads to the large- $\tilde{\lambda}$ behavior $\Gamma_\lambda \sim \tilde{\lambda}^3$ as well as the small- $\tilde{\lambda}$ behavior $\Gamma_\lambda \sim \tilde{\lambda}^5$.

Before concluding our discussion of the decay widths, it is important to note that there will generally exist many competing decay modes for our KK states which do not exclusively involve Standard-Model particles as end-products. One example includes intra-ensemble decays (*i.e.*, decays *within* the KK tower, from heavier KK states to lighter KK states); indeed, this possibility will be discussed in general terms in the Appendix. Also, in cases involving multiple fields in the bulk, it is possible for bulk KK states of one species to decay to bulk states of another species.

While such decays can be important on a number of cosmological and phenomenological levels, they generally do not significantly diminish the abundance of what might be termed “dark matter” or increase the corresponding abundance of what might be termed “visible matter”. Moreover, it is often the case that such decays are significantly suppressed relative to the KK decays

that proceed directly to Standard-Model brane states. Such suppressions can occur for a variety of reasons, some of which depend on the fact that physics in the bulk is often governed directly by (and therefore suppressed by) the gravitational Planck scale, and some of which are the consequences of extra restrictive symmetries which exist purely in the bulk and which therefore do not apply to decays of bulk fields into brane fields. Of course, a detailed analysis of this question requires specifying a particular bulk field, along with a complete Lagrangian for the theory including its gravitational interactions. While such an analysis is beyond the scope of this theoretical overview, an analysis of this sort does appear in Refs. [6, 7] where it is shown that such decays are indeed greatly suppressed in a specific realistic model of dynamical dark matter. This result therefore confirms our general expectations in one specific example.

We have therefore assumed in this paper that the primary decay mode for each KK bulk mode is directly into a Standard-Model brane state. However, as discussed in the Appendix, our dynamical dark-matter scenario can easily be generalized to accommodate more complex decay channels if this should ultimately prove appropriate in a given situation.

3. Balancing lifetimes against abundances

Having calculated the spectrum of abundances Ω_λ and the spectrum of decay widths Γ_λ across our KK tower, we can now see exactly how KK towers manage to balance lifetimes against abundances. Combining the results in Eqs. (63) and (72), we find that for large λ our KK towers indeed always obey a balancing equation of the form anticipated in Eq. (28):

$$\begin{aligned} \text{instantaneous :} & \quad \Omega_\lambda \Gamma_\lambda^{2/3} \sim \text{constant} \\ \text{staggered (RD era) :} & \quad \Omega_\lambda \Gamma_\lambda^{7/6} \sim \text{constant} \\ \text{staggered (RH/MD eras) :} & \quad \Omega_\lambda \Gamma_\lambda^{4/3} \sim \text{constant} . \end{aligned} \quad (73)$$

Indeed, this asymptotic behavior holds for $\tilde{\lambda} \gg \sqrt{1 + \pi^2/y^2}$. Thus, we see that our KK towers succeed in balancing lifetimes against abundances in a robust fashion, regardless of the particular type of “turn-on” they experience and regardless of the cosmological era during which this “turn-on” takes place.

While Eq. (73) describes the crucial asymptotic behavior at the “top” of the KK tower, a similar set of relations describes the “bottom” of each KK tower. Combining the small- $\tilde{\lambda}$ behavior in Eq. (64) with the small- $\tilde{\lambda}$ result $\Gamma_\lambda \sim \tilde{\lambda}^5$ leads to the relations

$$\begin{aligned} \text{instantaneous :} & \quad \Omega_\lambda \sim \text{constant} \\ \text{staggered (RD era) :} & \quad \Omega_\lambda \Gamma_\lambda^{3/10} \sim \text{constant} \\ \text{staggered (RH/MD eras) :} & \quad \Omega_\lambda \Gamma_\lambda^{2/5} \sim \text{constant} \end{aligned} \quad (74)$$

for $\tilde{\lambda} \ll \sqrt{1 + \pi^2/y^2}$. We stress, however, that this behavior is relevant only at the bottom of a KK tower, and only for relatively small y . Indeed, regardless of the value of y , the behavior of the abundances and decay widths always eventually shifts to satisfy the relations in Eq. (73) as we pass to higher and higher modes in a given KK tower.

Given these results for the abundances Ω_λ and decay widths Γ_λ , we can now calculate the general (α, β) scaling coefficients that appear in Eq. (15). These results also enable us to deduce an “effective” equation of state for our ensemble of decaying dark-matter KK components. The values of α , of course, are directly evident from Eq. (73) for large $\tilde{\lambda}$ and from Eq. (74) for small $\tilde{\lambda}$. Likewise, since the states in our KK tower are nearly equally spaced throughout the tower, we know that the density of states per unit λ is essentially λ -independent: $n_\lambda \sim \lambda^0$. Per unit of Γ , this translates into $n_\Gamma \sim n_\lambda |d\Gamma/d\lambda|^{-1} \sim \Gamma^{(1-x)/x}$ for $\Gamma \sim \lambda^x$. We thus have $\beta = -2/3$ for large λ , and $\beta = -4/5$ for small λ .

We therefore conclude that for large λ , a general KK tower has the scaling coefficients

$$(\alpha, \beta) = \begin{cases} (-2/3, -2/3) & \text{instantaneous} \\ (-7/6, -2/3) & \text{staggered (RD era)} \\ (-4/3, -2/3) & \text{staggered (RH/MD eras)} \end{cases}. \quad (75)$$

By contrast, for small $\tilde{\lambda}$, these results are modified to become

$$(\alpha, \beta) = \begin{cases} (0, -4/5) & \text{instantaneous} \\ (-3/10, -4/5) & \text{staggered (RD era)} \\ (-2/5, -4/5) & \text{staggered (RH/MD eras)} \end{cases}. \quad (76)$$

Given these (α, β) scaling coefficients, we can also calculate the effective equation-of-state function $w_{\text{eff}}(t)$ which describes the collective effects of the decays of the individual modes along the KK tower. Indeed, as we have seen in Sect. II, the behavior of this function $w_{\text{eff}}(t)$ depends critically on the value of the sum $x \equiv \alpha + \beta$. However, given the results in Eqs. (75) and (76), we can easily tabulate the values of x for the different cases under study, obtaining the results shown in Table I. As we see from Table I, most of the x -values for a general KK tower tend to cluster near $x \lesssim -1$. *This is remarkable, since we have already shown in Sect. II that this is precisely the range for x which is preferred phenomenologically.* We thus see that a KK tower indeed serves as an excellent realization of dynamical dark matter.

One feature which emerges from Table I is that regardless of the turn-on behavior of the individual modes, the value of x generally decreases as we pass from the large- $\tilde{\lambda}$ regime to the small- $\tilde{\lambda}$ regime. This generally corresponds to passing from early times (during which the decays of the heavier KK modes dominate the physics) to later times (during which only the lighter KK modes are still present). Indeed, this transition typically occurs for values of $\lambda \sim \sqrt{1 + \pi^2/y^2}$ which decrease as a function of y . Thus, we do not expect to see the small- $\tilde{\lambda}$ behavior

| | large $\tilde{\lambda}$ | small $\tilde{\lambda}$ |
|------------------------|-------------------------|-------------------------|
| instantaneous | -4/3 | -4/5 |
| staggered (RD era) | -11/6 | -11/10 |
| staggered (RH/MD eras) | -2 | -6/5 |

TABLE I: Values of the equation-of-state parameter $x \equiv \alpha + \beta$ for different portions of a general KK tower with different “turn-on” phenomenologies. We observe that KK towers naturally give rise to values $x \lesssim -1$, which is precisely the range favored phenomenologically.

emerge strongly except for later times in small- y scenarios.

Needless to say, all of the above conclusions are predicated on approximations which model the KK tower according to certain power-law scaling behaviors. It is therefore natural to wonder how robust these conclusions actually are when compared with the results of a complete numerical calculation which uses the exact numerical values for the eigenvalues $\tilde{\lambda}$ across the entire KK tower and which avoids any approximations for the coefficients A_λ which appear in the KK mode abundances and decay widths. However, it is straightforward to perform such a calculation. In Fig. 6, we plot a rescaled version of the total dark-matter abundance Ω_{tot} as a function of time during its final decay-dominated period, assuming (as in Sect. II) that these decays occur during the present matter-dominated cosmological era. Each panel in Fig. 6 corresponds to one of the three different cases that describe how the individual abundances in the KK tower might have been established; indeed, following the results in Eq. (61), this “rescaled” Ω_{tot} is defined in each case as $\sum_\lambda \tilde{\lambda}^k A_\lambda^2 X_\lambda$ with $k = 2$ (first panel of Fig. 6), $k = 1/2$ (second panel), and $k = 0$ (third panel). Moreover, in making these plots, we have assumed that each KK state decays instantaneously at $t = \tau_\lambda \equiv \Gamma_\lambda^{-1}$ so that the contributions from individual states will be readily discernible. This is tantamount to approximating X_λ in Eq. (55) as $X_\lambda(t) \approx \Theta(\Gamma_\lambda^{-1} - t)$. Finally, in order to compare curves with different values of y , an overall normalization for the time axis for each curve has been chosen such that the time t is expressed in units of Γ_0^{-1} , where Γ_0 is the decay width of the lightest KK mass eigenstate. As a result the curves in Fig. 6 share a common location at which Ω_{tot} ultimately vanishes in each case, signifying the eventual decay of the final, lightest state in the KK tower.

Although the total dark-matter abundance Ω_{tot} ultimately vanishes at $\log(\Gamma_0 t) = 0$ for all curves, we see that the overall time-evolution of Ω_{tot} as we approach this vanishing point is highly y -dependent. As $y \rightarrow \infty$, we see that Ω_{tot} remains constant until it experiences a single, sudden, complete decay; this of course corresponds to the traditional scenario of a single dark-matter particle. By contrast, for smaller values of y , we see that multiple modes with different decay widths carry the total dark-matter abundance Ω_{tot} ; as a result, the resulting

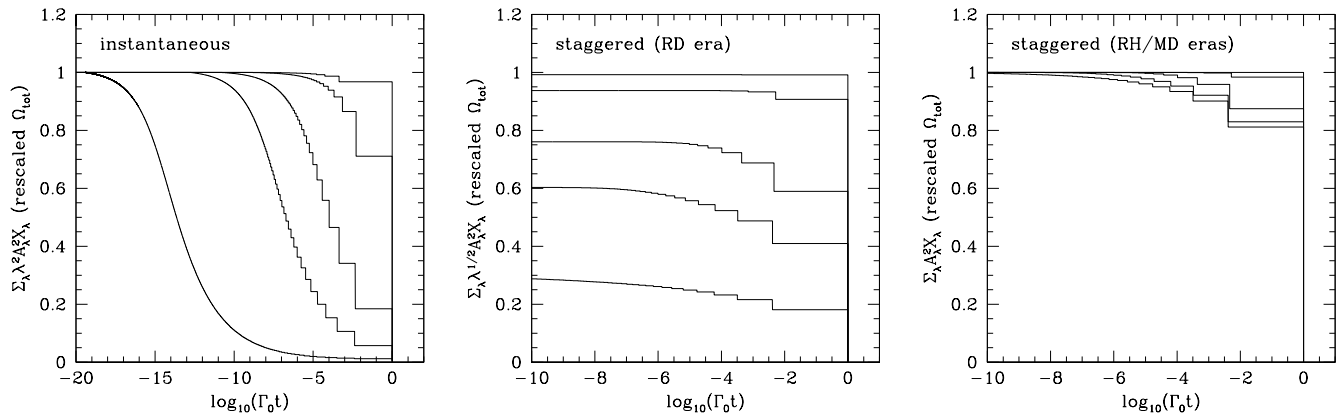


FIG. 6: The (rescaled) total dark-matter abundance Ω_{tot} , plotted as a function of time for each of the three cases relevant for a general KK tower. In each panel, the uppermost curve corresponds to $y = 10$ and the successively lower curves correspond to $y = 3$, $y = 1$, $y = 0.5$, and $y = 0.1$. In order to compare curves with different values of y , we have plotted $\log_{10}(\Gamma_0 t)$ on the horizontal time axis, where Γ_0 is the decay width of the lightest KK mass eigenstate associated with each curve. This ensures that the curves share a common horizontal location at which Ω_{tot} vanishes in each case, signifying the decay of the final, lightest state in the KK tower. We see from these results that overall shape of the time-dependence of Ω_{tot} is highly y -dependent: the $y \rightarrow \infty$ limit corresponds to the usual scenario of a single dark-matter particle (with Ω_{tot} remaining essentially constant until this particle decays), while smaller values of y correspond to situations in which Ω_{tot} is distributed across multiple KK modes with different decay widths. It is this property which leads to a time-dependent Ω_{tot} and thus a non-trivial “effective” equation of state for the dark KK tower.

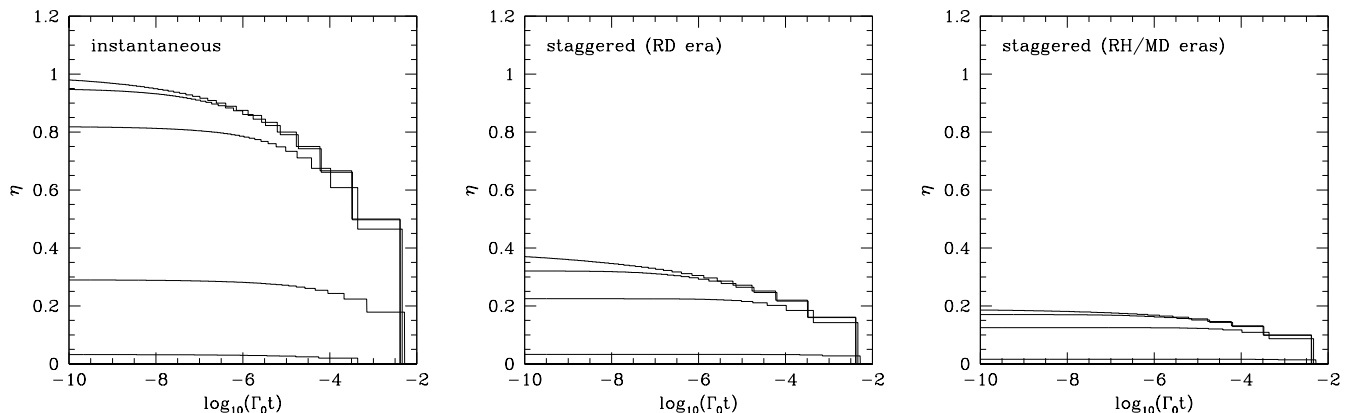


FIG. 7: The tower fraction η , plotted as a function of time for each of the three cases relevant for a general KK tower. In each panel, the lowest curve corresponds to $y = 10$ (not visible in the center and right panels) and the successively higher curves correspond to $y = 3$, $y = 1$, $y = 0.5$, and $y = 0.1$. Thus, these values for η directly correspond to the values of Ω_{tot} plotted in Fig. 6. In general, we observe that η increases with decreasing y , and that the maximum value of η shown for each curve is consistent with the results of Fig. 5.

transition of Ω_{tot} from its maximum value to zero is more gentle. In all cases the quantity $1 - \eta$ indicates the relative size of this final “last step” down to $\Omega_{\text{tot}} = 0$; note that the results for η implicitly shown here in terms of the relative final step size are consistent with those shown in Fig. 5. Likewise, the *initial* values of Ω_{tot} also confirm our expectations discussed earlier: the instantaneous and staggered (RH/MD) cases have initial values at $\Omega_{\text{tot}} = 1$, in accordance with Eq. (65) for all y , while the initial values shown on the second panel are y -dependent and correspond to the values shown in Fig. 4.

Using the results for $\Omega_{\text{tot}}(t)$ shown in Fig. 6, we can now proceed to calculate the corresponding tower frac-

tions $\eta(t)$. The results are shown in Fig. 7. As expected, we see that η increases with decreasing y . Moreover, we can now see directly that the maximum value of η shown for each curve is consistent with the results of Fig. 5.

Using the results for $\Omega_{\text{tot}}(t)$ shown in Fig. 6, we can also proceed to calculate the corresponding equation-of-state function $w_{\text{eff}}(t)$ which follows from the definition in Eq. (7). Equivalently, we can use the results for $\eta(t)$ shown in Fig. 7 along with the definition in Eq. (9). In either case, the results are shown in Fig. 8. In passing from Figs. 6 and 7 to Fig. 8, we have calculated logarithmic slopes numerically for each successive KK decay event and then plotted a continuous function. It is clear

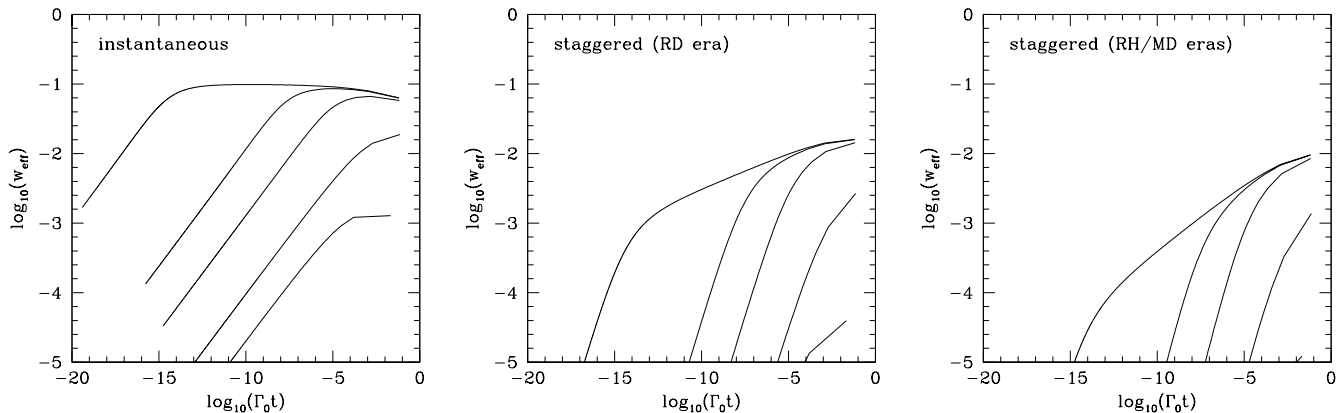


FIG. 8: The effective dark-matter equation-of-state parameter w_{eff} , plotted as a function of time for each of the three cases relevant for a general KK tower. In each panel, the lowest curve corresponds to $y = 10$ and the successively higher curves correspond to $y = 3$, $y = 1$, $y = 0.5$, and $y = 0.1$. Thus, these values for w_{eff} directly correspond to the values of Ω_{tot} plotted in Fig. 6, or equivalently the values of η plotted in Fig. 7. In all cases, we see that $w_{\text{eff}} \rightarrow 0$ as $t \rightarrow 0$. Note that although the values of Ω_{tot} were plotted in Fig. 6 only up to an overall rescaling factor, the values of w_{eff} plotted here are insensitive to this rescaling and are thus meaningful on an absolute scale. We thus see that w_{eff} never exceeds 0.1 for a general KK tower, and is generally much smaller.

that the results in Fig. 8 are in complete agreement with our general expectations for w_{eff} from Sect. II: in each case we observe the general tendency that $w_{\text{eff}} \rightarrow 0$ as $t \rightarrow 0$, and likewise in all but one case w_{eff} approaches a pole at $t = \Gamma_0^{-1}$ (corresponding to the fact that Ω_{tot} hits zero upon the decay of the final, lightest dark-matter mode in the KK tower).

These results are also in agreement with our expectations based on the KK scaling coefficients in Table I. As y decreases, we see the emergence of a definite shift in the behavior of $w_{\text{eff}}(t)$ as we transition from early times to later times. This corresponds to the shift from large- $\tilde{\lambda}$ behavior to small- $\tilde{\lambda}$ behavior in Table I. Indeed, in the case of an “instantaneous” turn-on, we even observe that our function $w_{\text{eff}}(t)$ develops a slight *maximum* for smaller values of y , shifting from increasing behavior to slightly decreasing behavior. This change in the slope of $w_{\text{eff}}(t)$ for this particular situation is directly correlated with the fact that the value of x in Table I shifts from $x < -1$ to $x > -1$. We see from both Table I and Fig. 8 that this is the only case in which such interesting behavior occurs.

At first glance, it might seem surprising that we are able to obtain effective equation-of-state functions $w_{\text{eff}}(t)$ which depend on x , but which are otherwise universal when plotted versus $\Gamma_0 t$. Indeed, $w_{\text{eff}}(t)$ depends on a number of parameters: not just the dimensionless exponents α and β in Eq. (15), but also dimensionful quantities such as the leading coefficients A and B in Eq. (15) as well as physical parameters such as Ω_{CDM} which are involved in setting a boundary condition for Ω_{tot} . Indeed, all of these parameters appear in our approximate results for $\Omega_{\text{tot}}(t)$ in Eqs. (18) and (19). However, the important point is that while Ω_{tot} depends on all of these dimensionful quantities somewhat independently, $w_{\text{eff}}(t)$ depends on them in only one particular combination. This was

already apparent in Eqs. (20) and (23), where the combination in question was nothing but $w_* \equiv w_{\text{eff}}(t_{\text{now}})$.

Of course, the results for $w_{\text{eff}}(t)$ in Eqs. (20) and (23) were respectively derived from the results for $\Omega_{\text{tot}}(t)$ in Eqs. (18) and (19), and these in turn were realized by taking our boundary condition to be $\Omega_{\text{tot}}(t_{\text{now}}) = \Omega_{\text{CDM}}$. However, we can equivalently write our boundary condition in the form $\Omega_{\text{tot}}(1/\Gamma_0) = 0$, where we are assuming that each KK mode with mass λ decays promptly at $t = \tau_\lambda \equiv \Gamma_\lambda^{-1}$, with Γ_0 denoting the width of the lightest mass eigenmode. Following the same algebraic manipulations as in Sect. II then leads to equations of state which are written in terms of Γ_0 rather than w_* :

$$w_{\text{eff}}(t) = \begin{cases} \frac{1}{2}(x+1) [1 - (\Gamma_0 t)^{x+1}]^{-1} & \text{for } x \neq -1 \\ \frac{1}{2}(\Gamma_0 t)^{-1} & \text{for } x = -1 \end{cases} \quad (77)$$

where $x \equiv \alpha + \beta$. Thus, when expressed in terms of the dimensionless time variable $\Gamma_0 t$ as in Fig. 8, our $w_{\text{eff}}(t)$ -functions are indeed universal, depending only on x .

It is important to bear in mind that in this section we have made only minimal assumptions concerning the precise nature of this KK tower or the identity of the fields it represents. We therefore expect that all of the features we have discussed in this section will hold quite generally, regardless of the identity of the particular field(s) which happen to populate the bulk and constitute the KK tower.

IV. DYNAMICAL DARK MATTER: NOVEL SIGNATURES AND PHENOMENOLOGICAL CONSTRAINTS

Having described the general theoretical structure of our dynamical dark-matter framework, we now present several additional features of this framework which are likely to be of importance in enabling this framework to satisfy phenomenological constraints. As in other sections, our discussion here will be restricted to broad, model-independent themes, and we shall present a detailed phenomenological analysis of one specific dynamical dark-matter scenario in Refs. [6, 7].

It turns out that there are three phenomenological features which are unique to dynamical dark matter, and which under certain circumstances might be taken as signatures (or even “smoking guns”) of the overall framework.

- *No well-defined dark-matter mass or cross-section:* First, since the dark-matter “candidate” within the dynamical dark-matter framework is not a single particle, but rather an ensemble of particles, it does not have a specific mass or cross-section associated with it. This represents a marked difference relative to most other dark-matter proposals, and implies that the kinematics associated with the production and decay of dynamical dark matter is likely to be quite different from that associated with more traditional single-component dark matter. This could have dramatic consequences for collider phenomenology (and potentially for direct detection), and may also have a number of cosmological implications.
- *Coupling suppression for light modes:* Second, it is almost inevitable that the eventual phenomenological success or failure of specific dynamical dark-matter scenarios involving large extra dimensions will ultimately rest in part on the couplings between the dynamical dark matter in the bulk and the Standard-Model states on the brane. Such couplings are of critical importance because they govern the degree to which this dark matter might be “visible” to the Standard Model. From intuitions based on studies of KK graviton dynamics, one might suspect that all mass eigenstates in the bulk would couple to the brane with equal strength. However, it turns out that the opposite is true for theories with a brane mass: while the most of the couplings between the fields on the brane and the mass eigenstates in the bulk are indeed uniform, the couplings between the brane and the *lightest* mass eigenstates in the bulk are significantly suppressed. We have already seen this behavior in Fig. 3, where we plot the coupling matrix element $\langle \phi_\lambda | \phi' \rangle = \tilde{\lambda}^2 A_\lambda^2$ as a function of λ : although this coupling always reaches an asymptotic value for sufficiently large λ , this coupling is significantly

suppressed for small λ . Indeed, the magnitude of this suppression can be controlled by varying the non-diagonality parameter y .

This suppression feature is of immense phenomenological importance, since the couplings of the lightest dark-matter eigenstates to the brane are precisely those which are the most dangerous for the viability of our dynamical dark-matter framework. Thus, this suppression feature can be very important in relaxing numerous phenomenological bounds on dynamical dark matter, and thereby constitutes an unexpected additional effect which can help dynamical dark matter stay dark despite its multitude of states.

- *Decoherence:* Finally, there is an additional feature associated with dynamical dark matter in large extra dimensions which can play an important role in its phenomenology: this is the phenomenon of “decoherence” [11]. As we have seen in Sect. III, only one particular linear combination of bulk dark-matter modes ϕ_n can couple to the brane: this is the linear combination ϕ' . However, once ϕ' is created through an interaction with the brane, it rapidly *decoheres* as it propagates because it is not a mass eigenstate.

One way to understand this decoherence involves simple quantum mechanics: because ϕ' consists of a huge number of different mass eigenstates, and because the masses of these eigenstates are generally not related to each other through rational multiplicative factors, the different mass eigenstates fall out of phase with each other under time-evolution and will not reconstitute ϕ' within finite time. Thus, they cannot couple to the brane at later times, and essentially become “invisible” as far as physics on the brane is concerned. Another (quantum field-theoretic) way to describe the same phenomenon is simply that the amplitude associated with any process that involves the production and subsequent detection of dark matter on the brane will have multiple individual contributions, each associated with the propagation of an intermediate state consisting of an individual dark-matter component. However, because these individual components have different masses, their corresponding amplitudes accrue different phases. These amplitudes therefore destructively interfere within the calculation of any cross-section sum.

This decoherence phenomenon can have important phenomenological consequences. Indeed, decoherence generically induces a suppression of the cross-section for any process involving virtual dark-matter particles by a factor of N , where N is the number of such particles being exchanged. This, then, is yet another mechanism which helps dynamical dark matter stay dark. We emphasize that this feature is not specifically extra-dimensional;

it applies to any dark-matter framework in which the dark matter has many components of different masses, and in which only a specific linear combination of those components can couple to Standard-Model states.

Needless to say, dynamical dark matter must ultimately be subjected to all of the phenomenological bounds and constraints that apply to more traditional dark-matter candidates. However, because dynamical dark matter consists of a vast ensemble of individual states which are not necessarily stable on cosmological time scales, many of these constraints take unusual forms in this context. We shall therefore now provide a quick overview of the different classes of laboratory, astrophysical, and cosmological constraints which apply to dark matter in general, and then indicate the forms they can be expected to take within the context of dynamical dark matter. Once again, we emphasize that our goal here is merely to provide a model-independent theoretical overview in which we restrict ourselves to addressing a single question: *for each class of constraints that apply to theories of dark matter, what combinations of parameters are bounded in the traditional framework and how do these combinations translate into our dynamical dark-matter framework?* Explicit details concerning a particular dynamical dark-matter scenario can be found in Refs. [6, 7].

Broadly speaking, there are four classes of constraints which apply to any candidate theory of dark matter.

- First, there are general constraints on the relic dark-matter abundance and on the dark-matter equation of state. The constraints on the dark-matter abundance $\Omega_{\text{tot}}(t)$ are similar to those which apply in traditional dark-matter scenarios: $\Omega_{\text{tot}}(t_{\text{now}})$ must match the observed dark-matter relic abundance Ω_{CDM} ; the dark-matter ensemble must not cause the universe to become matter-dominated too early; *etc.* However, our scenario differs from traditional dark-matter scenarios in that it gives rise to an equation-of-state-parameter w_{eff} which can be different from zero and which generally exhibits a non-trivial time dependence. Astrophysical and cosmological considerations therefore imply additional constraints on our equation-of-state function $w_{\text{eff}}(t)$, or equivalently on the scaling coefficients (α, β) .
- Second, there are constraints on dark matter which derive from physical processes in which dark matter is produced through its interactions with Standard-Model particles but not subsequently detected. For example, there are collider constraints on processes in which dark-matter particles manifest themselves as missing energy. Furthermore, if the dark-matter candidates in question are sufficiently light, additional constraints can be derived from limits on dark-matter production by astrophysical sources.

For example, dark-matter particles produced in stars and supernovae can carry away energy from these sources very efficiently. This can lead to observable effects on stellar lifetimes, energy-loss rates from supernovae, *etc.* Indeed, observational limits on the magnitudes of these effects imply stringent bounds on any light particle whose interactions with the Standard-Model fields are highly suppressed.

To see how such considerations constrain the parameters of a generic dark-matter model, let us consider a traditional single-component scenario in which the dark-matter candidate resides in a hidden sector. The dominant interaction between the dark sector and the Standard Model in such scenarios occurs through non-renormalizable operators \mathcal{O}_n of mass dimension n , suppressed by inverse powers of some large mass scale Λ associated with the cutoff of the theory. For example, Λ might be an effective Planck scale M_P in the case of dark-matter candidates associated with gravity, or a particle mass M_R in the case of candidates such as a right-handed neutrino, or a dynamical scale such as the Peccei-Quinn scale f_{PQ} in the case of axions. The cross-section for dark-matter production will therefore be suppressed by a factor of $\Lambda^{2(4-n)}$, and constraints in this class thus ultimately become constraints on Λ .

For example, in the specific dynamical dark-matter scenario presented in Sect. III, the leading operators have mass-dimension five, and Λ is equated with the suppression scale \hat{f}_ϕ . Thus, constraints in this class ultimately become bounds on $1/\hat{f}_\phi^2$. Or, phrased directly in terms of the decay widths and abundances which are the bedrock of our scenario, these constraints yield bounds on $\sum_\lambda \lambda^{-3}\Gamma_\lambda$, where the sum over mass eigenstates includes only those states which are kinematically relevant for the process in question.

We conclude, then, that constraints of this type tend to place bounds on the particular combination $\sum_\lambda \lambda^{-3}\Gamma_\lambda$. However, this quantity is significantly affected by the coupling-suppression effect discussed above. As a result, such bounds can often turn out to be considerably weaker than one might imagine at first glance.

- Third, there are constraints that arise from situations in which dark matter is produced through its interactions with Standard-Model particles and is then subsequently detected (either directly or indirectly) via those same interactions. Here we have in mind not only astrophysical production with subsequent detection on earth, but also any process involving virtual dark-matter particles. Which physical processes of this sort serve to constrain a particular dark-matter particle are extremely model-specific. Axions and other similar particles, for

example, are constrained primarily by helioscope searches, microwave-cavity experiments, *etc.*; other particles are more stringently constrained by collider limits, and so forth. Nevertheless, a few generic observations can be made.

If we assume, as above, that the dark matter resides in a hidden sector, it then follows that the cross-sections for processes of this sort are proportional to $\Lambda^{4(4-n)}$. Thus, once again, limits on such cross-sections ultimately become bounds on Λ . For example, in the specific dynamical dark-matter scenario presented in Sect. III, they become bounds on $1/\hat{f}_\phi^4$, or equivalently on the quantity $(\sum_\lambda \lambda^{-3}\Gamma_\lambda)^2$. In terms of overall mass scales, we might approximate this quantity as $\sum_\lambda \lambda^{-6}\Gamma_\lambda^2$, but we must also bear in mind that the cross-terms within such products can be significant. Indeed, these are precisely the situations in which the decoherence phenomenon discussed above can play a role. Thus, these constraints might also turn out to be significantly weaker than they might at first sight appear.

- Finally, there are constraints on dark-matter decays and annihilations. As far as decays are concerned, we have in mind constraints such as those from big-bang nucleosynthesis, measurements of the cosmic microwave background, observations of the diffuse X-ray and gamma-ray backgrounds, *etc.* The basic idea behind all of these constraints is that the decays of a cosmological population of dark-matter particles can result in measurable deviations from the standard cosmology at times $t \gtrsim 1$ s, or leave (unobserved) imprints on these backgrounds. In situations in which dark-matter annihilation cross-sections are sufficiently large, various additional limits (such as those from typical indirect-detection methods) would also apply.

Let us focus on those constraints related to dark-matter decays, as these are generic to dynamical dark-matter scenarios. (By contrast, constraints related to dark-matter annihilation tend to be somewhat model-dependent, and indeed often do not apply.) Roughly speaking, in a traditional single-component dark-matter scenario, such dark-matter decay constraints tend to place bounds on the product $\Omega_\chi\Gamma_\chi$, where Ω_χ and Γ_χ are the abundance and decay width of our dark-matter field χ , suitably evaluated during the appropriate cosmological period. In a dynamical dark-matter framework, by contrast, this now becomes a constraint on

$$\langle \Gamma \rangle \equiv \sum_\lambda \Omega_\lambda \Gamma_\lambda \quad (78)$$

where again our abundances and widths are to be evaluated during the cosmological epoch during which decays can contribute to the effect in question (the disruption of BBN, distortions of the

CMB, *etc.*). It is important to note that this dependence on time effectively truncates the range of the above sum to those states whose lifetimes fall roughly within the time scale associated with that epoch. Put another way, only those states whose masses lie within certain characteristic ranges contribute to the sum. Of course, at a mathematical level, the behavior of this sum ultimately depends critically on the balancing relations that happen to hold across the entire dark-matter ensemble. Note that these arguments will be addressed more rigorously in Refs. [6, 7].

Finally, for completeness, we also mention two further classes of constraints which must also be borne in mind. Unlike the previous constraints, these are substantially more model-dependent.

- First, there can be phenomenological bounds that accompany (and are therefore specific to) particular realizations of dynamical dark matter. For example, we have seen that an infinite tower of Kaluza-Klein states furnishes an excellent realization of dynamical dark matter. However, the extra-dimension brane/bulk framework brings with it a whole host of additional bounds and constraints, some of which come from the fact that we are now attempting to do standard physics within such a context (*e.g.*, the need for a late-time-reheating (LTR) cosmology [10]), and others of which place bounds on the context itself (*e.g.*, Eötvös-type or Cavendish-type “fifth-force” experiments which restrict the allowed sizes of the extra dimensions). Such constraints are clearly highly model-dependent, and frequently they are also wholly independent of the general dynamical dark-matter framework.
- Finally, there can also be constraints that arise simply for reasons of theoretical self-consistency. For example, if we assume (as we have done here) that our initial dark-matter abundances are determined through misalignment production, then we must insist that misalignment production indeed dominates over other production mechanisms such as thermal production. This, of course, yields a non-trivial constraint on the parameters of the model. Likewise, the assumption that dynamical dark matter in the bulk decays preferentially to Standard-Model states on the brane, rather than to other dynamical dark-matter states in the bulk, implies yet another self-consistency requirement. Once again, however, constraints in this class tend to be highly model-dependent and therefore do not represent generic constraints on the dynamical dark-matter framework.

This is clearly a fairly long list of constraints, and one must not minimize the impact that they can have in ruling out specific dark-matter proposals. In Refs. [6, 7],

however, we shall study one particular realization of dynamical dark matter, and we shall exhaustively work through all of the constraints relevant for this particular realization. We shall find that for this particular scenario, our dynamical dark-matter framework indeed survives all known laboratory, astrophysical, and cosmological constraints. This will thereby furnish us with an “existence proof” that dynamical dark-matter can indeed be a viable, alternative framework for addressing the central questions in dark-matter physics.

Finally, we remark that for some purposes it may also be interesting to consider the phenomenology associated with our overall dark-matter framework when the individual component decay widths Γ_i are extremely small. Of course, in the actual limit $\Gamma_i \rightarrow 0$ we know that Ω_{tot} approaches a constant in the final, matter-dominated era; likewise, $w_{\text{eff}} \rightarrow 0$. In this respect, this limit of our framework begins to resemble a traditional *non*-dynamical dark-matter framework, thereby allowing us to evade many of the most stringent phenomenological constraints coming from dark-matter decays in the early universe. However, even in this limit, our framework nevertheless continues to retain those distinctive features which stem from its underlying multi-component nature. For example, we can still have $\eta \neq 0$. We also still have the possibility of staggered turn-ons as well as the possibility of coupling suppression for light modes. We even continue to have decoherence, even though many of the processes for which decoherence is most phenomenologically relevant will already tend to be suppressed in the $\Gamma_i \rightarrow 0$ limit. And perhaps most importantly, the dark matter in our framework will continue to evade simple characterization in terms of a single well-defined mass or cross-section.

Needless to say, we are not particularly interested in the limit $\Gamma_i \rightarrow 0$. Indeed, we regard the dynamical aspects of our dark-matter framework to be among its most intriguing features and key signatures. However, the freedom to tune the values of Γ_i relative to the other dimensional parameters in our framework is important from a theoretical standpoint because it illustrates that our overall dark-matter framework possesses a means of “dialing” the scale associated with its dynamical aspects relative to those associated with its multi-component aspects. This is particularly relevant because the dynamical aspects of our framework are often ultimately subject to an entirely different set of phenomenological bounds and constraints than those governing its multi-component aspects. Thus, the freedom to independently adjust the scales associated with these different aspects of our dark-matter framework gives this framework an added flexibility when it comes to satisfying many of the phenomenological bounds discussed above.

Of course, within the particular higher-dimensional brane/bulk context discussed in Sect. III, this freedom may initially appear to be lacking: a single five-dimensional mass scale f_Φ governs not only the magnitudes of the abundances of individual dark-matter com-

ponents but also the magnitudes of their corresponding decay widths. Indeed, in particular realizations of this framework, even the brane mass m can be tied to f_Φ , and we shall see an explicit example of this in Ref. [6]. However, there is in principle no reason why the mass scale f_Φ which appears in Eq. (47) and which ultimately sets the scale for dark-matter abundances needs to be the same as the mass scale f_Φ which appears in Eqs. (68) and (69) and which ultimately sets the scale for decay widths. Indeed, identifying these two quantities is merely a minimal assumption about the energy scales in our higher-dimensional theory, and we can easily envision more complex scenarios in which these two mass scales are significantly different.

V. CONCLUSIONS AND DISCUSSION

In this paper, we have introduced a new framework for dark-matter physics which we call “dynamical dark matter”. Unlike most approaches to the dark-matter problem which hypothesize the existence of a single, stable, dark-matter particle, our dynamical dark-matter framework may be characterized by the fact that the requirement of stability is replaced by a delicate balancing between cosmological abundances and lifetimes across a vast ensemble of individual dark-matter components. This setup therefore collectively produces a time-varying cosmological dark-matter abundance, and decays of the different dark-matter components can occur continually throughout the evolution of the universe.

Although our framework is quite general and need not be tied to a specific set of particles or theoretical models, we have shown that one natural realization of this scenario consists of a tower of KK states corresponding to a single higher-dimensional field propagating in the bulk of large extra spacetime dimensions. Indeed, as we have shown, the states in such a “dark tower” naturally obey inverse “balancing” equations that relate their abundances and decay widths in just the right manner. Remarkably, this remains true even if the stability of the KK tower itself is entirely unprotected. Our dynamical dark-matter scenario is therefore well-motivated both in field theory and string theory, and can even be used to constrain the cosmological viability of certain limits of string theory. We have also seen that within this context, dynamical dark matter generically gives rise to certain phenomena such as coupling suppression and decoherence which may help to explain why dark matter is dark and thus far unobserved. Such phenomena transcend those usually associated with traditional single-component dark matter, and may in some sense be viewed as unique signatures for a dark-matter framework such as ours which rests on the existence of a large multitude of individual dark-matter components.

Needless to say, there are many possible generalizations of our basic dynamical dark-matter framework. Some of these apply to dynamical dark matter in general, while

others are more specific to realizations involving extra dimensions. For example, insofar as our general dark-matter ensemble is concerned, there are several natural extensions which can be contemplated.

- Not all components within the ensemble need be scalars. Higher-spin fields may also be considered. We may even demand that our ensemble be supersymmetric, although there would be no obvious need for R -parity within such supersymmetric extensions as far as dark-matter considerations are concerned.
- In this paper, we have examined the case of relatively simple dimension-five couplings between the components in the ensemble and the fields of the Standard Model. However, different scenarios may involve different coupling structures, and thus different models will lead to their own distinctive phenomenologies.
- Continuing along these lines, we have assumed in this paper that all of the components of our dynamical dark-matter ensemble are neutral under the Standard-Model gauge symmetries. While this choice is particularly convenient, allowing the possibility of specific realizations of our scenario in higher-dimensional brane/bulk Kaluza-Klein theories, there is nothing intrinsic to the dynamical dark-matter framework that requires this to be the case. In particular, some or all of the components of our dark-matter ensemble could have $\mathcal{O}(1)$ $SU(2)$ weak interactions with the Standard Model. This would, of course, undoubtedly tighten many of the phenomenological constraints on such scenarios; likewise, scattering processes involving such dark-matter components are also generally likely to play an important role and would need to be included in the analysis along the lines discussed in the Appendix. However, as long as the lifetimes of the ensemble components are sufficiently balanced against their abundances, the basic features of our framework will remain intact.
- In this paper, we have considered all decays of our ensemble components to be essentially instantaneous. However, such decays really have an exponential time-dependence. The fact that these decays have different widths can thus lead to further non-trivial effects on the time-dependence of the total dark-matter abundance associated with the ensemble.
- The primary decay mode for a given dark-matter component within our ensemble need not always be directly into Standard-Model states. In particular, it is also possible to consider decays from heavier ensemble components into lighter ensemble components. Note that in this sense, we are viewing the ensemble as consisting of all states which

are neutral under Standard-Model symmetries, including fields which reside in what might in more traditional contexts be considered a hidden sector. Such intra-ensemble decays could significantly alter the sorts of balancing equations which might arise across our dynamical ensemble, and as we shall discuss in the Appendix, they can thereby modify the time-dependence associated with Ω_{tot} , η , and w_{eff} .

- Misalignment production need not be the only mechanism through which the abundances of our individual components are initially established. Many other mechanisms (*e.g.*, thermal production, decays arising from topological defects, *etc.*) also provide ways of populating the different components, and can likewise lead to different resulting phenomenologies for dynamical dark matter. In particular, it would be very interesting (and relevant for our overall framework) to see whether the correct sorts of balancing relations might arise for situations in which our different ensemble components are populated in the manner of a standard WIMP — *i.e.*, by thermal freeze-out.
- At many points in this paper, we have made assumptions that simplify our analysis. For example, in Sect. II we have assumed that t_1 , the time by which our staggered turn-on has ended, is less than t_2 , the time at which significant dark-matter decays commence. Likewise, we have assumed for much of our analysis of abundances in Sect. III that a staggered turn-on, if it occurs, takes place entirely within a single epoch (either RH, RD, or MD). While such assumptions prove useful for analyzing the effects of different features of our framework individually, there is nothing intrinsic to the dynamical dark-matter framework which requires that these features be separated in this way, and numerous extensions and combinations of these features are possible.
- Although we have discussed several different signatures which are unique to dynamical dark matter, it is likely that our discussion has only begun to scratch the surface. It would be interesting to investigate what other kinds of signatures are also possible within this framework.
- Finally, our discussion in this paper has assumed a standard FRW cosmology. However, it would be interesting to repeat this analysis for a Λ CDM cosmology (and also for versions thereof with low reheat temperatures, as appropriate for theories with large extra dimensions). Indeed, within such cosmologies, quantities such as Ω_{tot} will experience additional types of time-dependence beyond those considered here.

Likewise, within the specific framework of large extra dimensions in which our dynamical ensemble of dark-matter components is represented by an infinite tower of

Kaluza-Klein states, there are also numerous generalizations and extensions which may be contemplated.

- We may consider situations involving multiple species of bulk fields. For example, the bulk can be a crowded place, consisting of a whole plethora of particles which are neutral under all Standard-Model gauge symmetries: these include gravitons and gravitini, axions and other axion-like particles, string-theory moduli, right-handed neutrinos, and so forth. From the point of view of physics on the brane, all of these states can be considered “dark matter”, and their contributions to quantities such as Ω_{tot} must all be considered within the overall dynamical dark-matter framework.
- We also need not restrict ourselves to a single extra spacetime dimension. Multiple extra dimensions are also possible.
- Likewise, our extra dimensions need not necessarily be flat. Warped extra dimensions will give rise to an entirely different KK spectroscopy, and as a result the phenomenology of dynamical dark matter within such contexts is likely to be significantly different from what has been presented here.

The above represent ideas for generalizing our overall dynamical dark-matter scenario. However, it may also be possible to use this kind of dynamical framework in order to address questions that go beyond dark matter *per se*. While some of these are relatively straightforward, others are indeed quite speculative.

- One of the key features of dynamical dark matter is that quantities such as Ω_{tot} are *dynamical* (*i.e.*, time-dependent) in this framework — even during the current matter-dominated epoch during which the dark-matter abundance is normally thought to be roughly constant. It is therefore possible that such a dynamic approach could serve as a starting point towards addressing the cosmic coincidence problem.
- Further along these lines, it might also be possible to address the cosmological constant within a similar framework. For example, the energy density associated with each scalar field ϕ_i prior to its “turn-on” behaves as dark energy rather than dark matter. Thus in this respect the cosmological constant in our framework is time-dependent as well, and this sort of dynamic cosmological constant might even persist into the current epoch if there continue to exist light scalar modes which have not yet turned on. In this case, the process of dark-matter decays would necessarily *overlap* with the process of a staggered turn-on, and one might be able to develop a consistent theory in which a vast ensemble of states gives rise to both dynamical dark matter and dynamical dark energy.

- The framework of dynamical dark matter might also provide a new means of placing phenomenological bounds on string theory (and in particular, on candidate string models). After all, string models are typically rife with “bulk” fields — even if their extra dimensions are compactified at or near the traditional Planck scale. Some of these fields (such as moduli) are model-dependent: they depend on the particular kind of compactification geometry employed in the construction of the candidate string model and their masses depend on the particular stabilization mechanisms, if any, which have been employed. By contrast, some of these fields are generically model-*independent*: these include all fields associated with the (super)gravity multiplet, such as the graviton, dilaton, other higher-form fields, and their possible superpartners. Indeed, if the Standard Model is restricted to a stack of D-branes within a given string construction, the corresponding “bulk fields” include *all* string states which do not couple to those branes.

While these fields are typically required for the self-consistency of the string, those that are massless require stabilization. Indeed, this is nothing but the standard moduli problem. However, depending on the specific cosmological properties of these fields, it is also true that their abundances must necessarily be considered as contributing either to the total dark energy or the total dark matter of the universe — even after they are stabilized. An analysis of their cosmological effects is then likely to run along the lines we have presented here, and the cosmological viability of the underlying candidate string model thus necessarily becomes an issue to be studied within a dynamical dark-matter (or dynamical dark-energy) framework. Indeed, in such cases our dark-matter ensemble could potentially include not only string KK modes, but also (a subset of) string oscillator modes and string winding modes.

- One central feature of our dynamical dark-matter scenario is the phenomenon in which an ensemble of decaying “stuff” with one equation of state collectively simulates “stuff” with a different equation of state. For example, in the specific dynamical dark-matter scenario presented here, an ensemble of decaying dark-matter states (*i.e.*, each with $w = 0$) collectively simulates an effective equation of state with $w_{\text{eff}} > 0$. This notion of using a vast ensemble of states with one equation of state to simulate another is, we believe, worthy of exploration in its own right, independently of the specific uses for dark-matter physics that we have presented here.
- Further along the above lines, it is natural to ask whether we could construct an ensemble of individual components of “stuff” with *negative* w . The decays of these components within the ensemble

would therefore act to increase the effective value of w , and perhaps even simulate $w = 0$. In other words, it is possible that dark matter might not even need to be comprised of matter! In some sense, this is the converse of the scenario we have presented here, in which individual *matter* components collectively produce a value for w_{eff} which, though not too different from zero, is still non-zero. Indeed, both scenarios may represent equally legitimate approaches to the dark-matter problem.

- Pursuing these lines still further, one can even speculate as to whether an ensemble of decaying dark-energy components (each with $w = -1$) could simulate dark *matter* (with $w = 0$). Indeed, such individual dark-energy components need be nothing more complicated than a set of scalar fields ϕ_i which decay (potentially into a hidden sector) *prior* to turning on. Such an approach might then “unify” dark energy and dark matter as simultaneously stemming from a primordial ensemble of scalar fields.
- Along entirely different lines, there is another phenomenon inherent in our dynamical dark-matter framework which is potentially interesting in its own right: this is the phenomenon (discussed in Sect. III) in which a KK tower appears to have periodic modings for its heavier modes, but anti-periodic modings for its lighter modes. As we have seen in Sect. III, this result emerges rather generically, requiring only a bulk field that somehow accrues a non-zero brane mass. This phenomenon is extremely interesting, because one normally associates the modings of a given field with its boundary conditions around non-contractible loops in a topologically non-trivial space, or equivalently with the magnitudes of the fluxes which might penetrate those loops. This phenomenon therefore seems to suggest a mechanism by which such modings or fluxes might become effectively energy-dependent.
- Finally, the general phenomenon of decoherence is interesting in its own right. This might be extremely relevant for axion invisibility (see, *e.g.*, the discussion in Ref. [11]), and is also likely to be of more general applicability. Indeed, this might provide an interesting approach to the moduli problem in string theory, and explain why moduli such as the dilaton are not observed.

We see, then, that our dynamical dark-matter framework appears to be pregnant with numerous possibilities for extension and generalization. However, even as a framework for dark-matter physics, we caution that our presentation here has been limited to only the broadest model-independent theoretical aspects and features. In particular, it still remains to choose a specific realization of this scenario in terms of a particular species of bulk field, and examine the phenomenological consequences of

such a choice in complete detail. In other words, it still remains to build an actual *model* of dark matter within this framework. However, this is precisely what we shall do in Refs. [6, 7], and we shall verify there that our specific models satisfy all known collider, astrophysical, and cosmological constraints. We thus conclude that the dynamical dark-matter framework can indeed serve as a viable alternative to the standard paradigm of a single, stable, dark-matter particle, and that dynamical dark matter therefore has a legitimate place alongside other approaches to dark-matter physics.

Acknowledgments

We are happy to thank Z. Chacko, T. Tait, and N. Weiner for discussions. This work was supported in part by the Department of Energy under Grants DE-FG02-04ER-41291 and DE-FG02-04ER-41298. The opinions and conclusions expressed here are those of the authors, and do not represent either the Department of Energy or the National Science Foundation.

Appendix: Intra-ensemble decays

Throughout this paper, we have implicitly assumed that each component of our dark-matter ensemble preferentially decays directly into one or more Standard-Model states rather than into another, lighter component *within* the ensemble. In other words, we have been assuming that the decays associated with the widths Γ_i take the direct *extra-ensemble* form $\phi_i \rightarrow \text{SM}$, and that such direct decays dominate over all possible *intra-ensemble* decays which might produce other dark-matter components among their end-products. However, it is easy to generalize our overall framework to include cases in which this assumption is relaxed.

Towards this end, it proves useful to start by rewriting Eq. (3) in a more useful form. Recall that $\Omega_i \equiv \rho_i / \rho_{\text{crit}}$, where ρ_i is the energy density associated with our oscillating ϕ_i field and where $\rho_{\text{crit}} \equiv 3M_P^2 H^2$, where M_P is the reduced Planck mass. Eq. (3) can therefore be rewritten as

$$\dot{\rho}_i + (3H + \Gamma_i) \rho_i = 0. \quad (\text{A.1})$$

However, because this energy density ρ_i is entirely associated with the coherent oscillations of the (zero-momentum modes of the) scalar ϕ_i field, it is possible to repackage this energy density in terms of an effective number density $n_i \equiv \rho_i / m_i$. We then find

$$\dot{n}_i + (3H + \Gamma_i) n_i = 0. \quad (\text{A.2})$$

Indeed, Eq. (A.2) describes the evolution of the number densities associated with each of the oscillating components in our ensemble under the assumption that the only decays available for these components are direct decays

into Standard-Model states, *i.e.*, $\phi_i \rightarrow \text{SM}$, with widths Γ_i .

Let us now consider what happens if we introduce an additional set of intra-ensemble decays of the form

$$\phi_i \rightarrow \sum_j N_{ij}^{(\alpha)} \phi_j + X^{(\alpha)}. \quad (\text{A.3})$$

Here the α -index labels the specific decay channel, and $N_{ij}^{(\alpha)}$ are non-negative integers describing the multiplicities of the ϕ_j particles produced in this decay channel (each of which may be assumed to have $m_j < m_i$). Likewise, $X^{(\alpha)}$ collectively represents any fields *outside* our dark-matter ensemble (potentially including Standard-Model fields) which may also happen to be produced in this decay process. We shall let $\Gamma_i^{(\alpha)}$ denote the width associated with the decay in Eq. (A.3).

The inclusion of such additional decay channels into our discussion leads to two additional effects on the time-evolution of the number densities n_i . First, there will be an additional decline in n_i due to the new decay channels for ϕ_i which are now available. However, there is also the possibility of an *increase* in n_i due to the *production* of ϕ_i particles from the decays of presumably heavier components ϕ_j within the ensemble. Indeed, we find that Eq. (A.2) is now replaced with the *coupled* system of differential equations

$$\dot{n}_i + \left(3H + \Gamma_i + \sum_{\alpha} \Gamma_i^{(\alpha)} \right) n_i = \sum_j \left(\sum_{\alpha} N_{ji}^{(\alpha)} \Gamma_j^{(\alpha)} \right) n_j. \quad (\text{A.4})$$

In general, the solutions to Eq. (A.4) can exhibit a number of striking behaviors. Not only can there be direct decays into Standard-Model states, as before, but there can also be “cascade” decays that take place entirely within the dark-matter ensemble, from heavier states down to lighter states. Indeed, a given state can also decay directly into Standard-Model states at any point along the cascade. As a result, a particularly rich and subtle phenomenology can easily ensue depending on the relations between Γ_i and $\Gamma_i^{(\alpha)}$, with different portions of the ensemble exhibiting different particle-decay patterns in a manner reminiscent of the vacuum-decay patterns studied in Ref. [12]. The corresponding values of n_i can then alternatively rise and fall as time evolves.

The possibility of such dark-to-dark intra-ensemble decays also allows even more striking features to emerge. For example, once a given heavy state ϕ_i “turns on”, it can potentially decay to lighter states ϕ_k which, because of their relative lightness, have not yet turned on. Thus, in this way, we see that a given component ϕ_k within our ensemble can simultaneously contribute to dark matter (in the form of daughter particles from the decays of heavier dark-matter components ϕ_i); to “dark radiation” (if the momenta of these ϕ_k daughter particles are large compared to their masses); and to dark energy (in the form of the energy still trapped in the overdamped field ϕ_k).

Given the result in Eq. (A.4), it might seem at first glance to be a straightforward exercise to obtain a corresponding set of coupled differential equations for the energy densities ρ_i and the abundances Ω_i . Indeed, all that would seem to be necessary would be to start with Eq. (A.4) in place of Eq. (A.2) and essentially reverse the process that led from Eq. (A.1) to Eq. (A.2). However, in going from Eq. (A.1) to Eq. (A.2) we needed to assume that all of the energy density ρ_i was in the form of coherent zero-momentum mode oscillations of the field ϕ_i , and this will no longer be true when intra-ensemble decays are possible. Indeed, the daughters ϕ_i which are produced through such intra-ensemble decays are literal particles — they have their own momenta and energies which are governed by the kinematics of the specific intra-ensemble decays which produced them. As a result, while it is still valid to discuss the time-evolution of a total number density n_i as in Eq. (A.4), we cannot simply identify $\rho_i = m_i n_i$ in order to obtain a corresponding set of equations for the energy densities ρ_i or abundances Ω_i .

In order to handle this calculation correctly, it is first necessary to express the relations in Eq. (A.4) in terms of the phase-space distributions $f_i(|\vec{p}_i|, t)$ [or equivalently $f_i(E_i, t)$, simply denoted f_i] associated with each field ϕ_i . This will essentially yield a Boltzmann equation which describes the time-evolution of these distributions. To do this, we observe that in general we may write

$$\begin{aligned} n_i &= \int \frac{d^3 \vec{p}_i}{(2\pi)^3} f_i \\ \Gamma_i &= \frac{1}{2E_i} \int [d\pi_a(1 \pm f_a)] [d\pi_b(1 \pm f_b)] \cdots |\mathcal{M}|^2, \end{aligned} \quad (\text{A.5})$$

where Γ_i is the width for a generic decay of the form $\phi_i \rightarrow a + b + \dots$, where \mathcal{M} is the corresponding matrix element (including an implicit Dirac δ -function to enforce momentum conservation), where the momentum-integration measures are given by $d\pi \equiv g d^3 \vec{p} / [(2\pi)^3 2E]$ with g signifying the number of associated degrees of freedom, and where the \pm signs are chosen positive for bosons and negative for fermions. The left side of Eq. (A.4) then takes the form

$$\int \frac{d^3 \vec{p}_i}{(2\pi)^3} \left[\dot{f}_i + \left(3H + \Gamma_i + \sum_{\alpha} \Gamma_i^{(\alpha)} \right) f_i \right] \quad (\text{A.6})$$

and the right side of Eq. (A.4) takes the form

$$\sum_{j,\alpha} N_{ji}^{(\alpha)} \int [d\pi_j f_j] \left\{ \prod_{k \neq i} [d\pi_k (1 + f_k)]^{N_{jk}^{(\alpha)}} \right\} [d\pi_i (1 + f_i)]^{N_{ji}^{(\alpha)}} [d\pi_X (1 \pm f_X)] |\mathcal{M}|^2 \quad (\text{A.7})$$

where \mathcal{M} is the matrix element for the decay $\phi_j \rightarrow \sum_k N_{jk}^{(\alpha)} \phi_k + X^{(\alpha)}$. Equating the $d^3 \vec{p}_i$ integrands in

Eqs. (A.6) and (A.7) then yields the result

$$\begin{aligned} \dot{f}_i + \left(3H + \Gamma_i + \sum_{\alpha} \Gamma_i^{(\alpha)} \right) f_i = \\ \frac{1 + f_i}{2E_i} \sum_{j,\alpha} N_{ji}^{(\alpha)} \int [d\pi_j f_j] \left\{ \prod_{k \neq i} [d\pi_k (1 + f_k)]^{N_{jk}^{(\alpha)}} \right\} \\ [d\pi_i (1 + f_i)]^{N_{ji}^{(\alpha)} - 1} [d\pi_X (1 \pm f_X)] |\mathcal{M}|^2 \end{aligned} \quad (\text{A.8})$$

where we have recognized that although there are in principle $N_{ji}^{(\alpha)}$ different ways of identifying an integrand with respect to $d^3\vec{p}_i$ within Eq. (A.7), each yields the same result and therefore any choice will suffice.

Eq. (A.8) is a set of coupled differential equations for the phase-space distributions f_i . Indeed, while Γ_i is independent of the f_i , the quantity $\Gamma_i^{(\alpha)}$ has a hidden dependence on all f_j for which $N_{ij}^{(\alpha)} \neq 0$. However, despite the complexity of this system of equations, our remaining task is conceptually easy: we simply begin with the distributions

$$f_i(|\vec{p}_i|, t_0) = 4\pi^3 m_i (\phi_i^{(0)})^2 \delta^3(\vec{p}_i) \quad (\text{A.9})$$

at the time t_0 when our abundances are initially established, and then use the results in Eq. (A.8) in order to evolve these distributions forward in time. Indeed, the initial distributions in Eq. (A.9) reflect nothing more than the assertion that the original state of

our ensemble consists of fields ϕ_i whose zero-momentum modes are displaced by some amount $\phi_i^{(0)}$ from their minima in field space, with a resulting energy density given by $\rho_i \equiv \frac{1}{2} m_i^2 (\phi_i^{(0)})^2$. While the time-evolution of the effective number densities n_i can then be obtained from Eq. (A.8) by integrating this equation with respect to the measure $\int d^3\vec{p}_i / (2\pi)^2$ [thereby reproducing Eq. (A.4)], the time-evolution of the corresponding energy densities ρ_i can be obtained from Eq. (A.8) by integrating Eq. (A.8) with respect to the alternative measure $\int [d^3\vec{p}_i / (2\pi)^3] E_i = \int [d^3\vec{p}_i / (2\pi)^3] \sqrt{|\vec{p}_i|^2 + m_i^2}$. This, then, provides us with the desired coupled differential equations for the energy densities ρ_i , from which it is then trivial to obtain the corresponding equations for the abundances Ω_i .

Needless to say, there are many caveats which must be borne in mind when applying this formalism. First, in general we must require that such intra-ensemble decays not produce daughter particles with great momenta, for then our dark matter would not be sufficiently cold. Likewise, although we have included the possibility of intra-ensemble decays in the above analysis, we have disregarded the possible contributions from *scattering* processes which also potentially involve our ensemble components. Indeed, this is generally an excellent approximation for gravitons, moduli, axions, and other fields which are very weakly coupled. We have also disregarded the effects of inverse decays.

-
- [1] For recent reviews, see, *e.g.*,
G. Jungman, M. Kamionkowski and K. Griest, Phys. Rept. **267**, 195 (1996) [arXiv:hep-ph/9506380];
K. A. Olive, arXiv:astro-ph/0301505;
D. Hooper, arXiv:0901.4090 [hep-ph];
N. Weiner, “Dark Matter Theory,” video lectures given at TASI 2009, http://physicslearning2.colorado.edu/tasi/tasi_2009/tasi_2009.htm;
J. L. Feng, Ann. Rev. Astron. Astrophys. **48**, 495 (2010) [arXiv:1003.0904 [astro-ph.CO]].
- [2] G. Servant and T. M. P. Tait, Nucl. Phys. B **650**, 391 (2003) [arXiv:hep-ph/0206071];
H. C. Cheng, J. L. Feng and K. T. Matchev, Phys. Rev. Lett. **89**, 211301 (2002) [arXiv:hep-ph/0207125].
- [3] I. Antoniadis, Phys. Lett. B **246**, 377 (1990);
I. Antoniadis, K. Benakli and M. Quiros, Phys. Lett. B **331**, 313 (1994) [arXiv:hep-ph/9403290].
- [4] K. R. Dienes, E. Dudas and T. Gherghetta, Phys. Lett. B **436**, 55 (1998) [arXiv:hep-ph/9803466]; Nucl. Phys. B **537**, 47 (1999) [arXiv:hep-ph/9806292];
arXiv:hep-ph/9807522.
- [5] T. Appelquist, H. C. Cheng and B. A. Dobrescu, Phys. Rev. D **64**, 035002 (2001) [arXiv:hep-ph/0012100].
- [6] K. R. Dienes and B. Thomas, “Dynamical Dark Matter: II. An Explicit Model,” arXiv:1107.0721 [hep-ph] (to appear in Phys. Rev. D).
- [7] K. R. Dienes and B. Thomas, arXiv:1203.1923 [hep-ph].
- [8] E. Komatsu *et al.* [WMAP Collaboration], Astrophys. J. Suppl. **180**, 330 (2009) [arXiv:0803.0547 [astro-ph]].
- [9] L. Randall and R. Sundrum, Phys. Rev. Lett. **83**, 3370 (1999) [arXiv:hep-ph/9905221].
- [10] N. Arkani-Hamed, S. Dimopoulos and G. R. Dvali, Phys. Lett. B **429**, 263 (1998) [arXiv:hep-ph/9803315]; Phys. Rev. D **59**, 086004 (1999) [arXiv:hep-ph/9807344].
- [11] K. R. Dienes, E. Dudas and T. Gherghetta, Phys. Rev. D **62**, 105023 (2000) [arXiv:hep-ph/9912455].
- [12] K. R. Dienes and B. Thomas, Phys. Rev. D **79**, 045001 (2009) [arXiv:0811.3335 [hep-th]].